3-29-2022

Transmission and Distribution Co-Simulation and Applications

Mohammad Asif Iqbal Khan
Florida International University, mkhan103@fiu.edu

FLORIDA INTERNATIONAL UNIVERSITY

Miami, Florida

TRANSMISSION AND DISTRIBUTION CO-SIMULATION AND APPLICATIONS

A dissertation submitted in partial fulfillment of the

requirements for the degree of

DOCTOR OF PHILOSOPHY

in

ELECTRICAL AND COMPUTER ENGINEERING

by

Mohammad Asif Iqbal Khan

2022

To: Dean John L. Volakis
College of Engineering & Computing

This dissertation, written by Mohammad Asif Iqbal Khan, and entitled Transmission and Distribution Co-Simulation and Applications, having been approved in respect to style and intellectual content, is referred to you for judgment.

We have read this dissertation and recommend that it be approved.

Arif Sarwat

Mohammad Rahman

Fahad Saeed

Sumit Paudyal, Major Professor

Date of Defense: March 29, 2022

The dissertation of Mohammad Asif Iqbal Khan is approved.

Dean John L. Volakis
College of Engineering & Computing

Andrés G. Gil
Vice President for Research and Economic Development
and Dean of the University Graduate School

Florida International University, 2022

DEDICATION

I am dedicating my work to my father, Mohammad Rashidun Nabi Khan and my mother, Monowara Begum who both always inspired me to become a better and learned person.

ACKNOWLEDGMENTS

First and foremost, I am extremely grateful to my supervisor, Dr. Sumit Paudyal for his invaluable advice, continuous support, and patience during my PhD studies. His immense knowledge and plentiful experience have encouraged me in all the time of my academic research and daily life. I would also like to thank Dr. Mads R. Almassalkhi and Dr. Sukumar Kamalasadan; my research collaborative project leads, for their technical support to my research. I would like to thank all members of my committee, Dr. Arif Sarwat, Dr. Mohammad Ashiqur Rahman and Dr. Fahad Saeed whose valuable advice helped me refine my works. I would also like to thank all the faculty & staff members of my department, my colleagues and friends whose constant support and wisdom helped me focus on work as well have a memorable time during my study and research at FIU. Finally, I would like to express my gratitude to my parents and sisters for their immeasurable sacrifice, continuous inspiration and support, who have constantly inspired me and supported me morally in this long journey. Special thanks to my eldest sister, Rafia Akhtar Khan and her family whose presence in the same city made it easier to handle stress using a family environment and thus, recharge. Last but not least, I want to thank my life partner, Sultana Mubarika Rahman Chowdhury for her continuous help and support towards me in completing this degree. Without tremendous understanding and encouragement from all of these great souls in the past few years, it would be impossible for me to complete my studies.

ABSTRACT OF THE DISSERTATION

TRANSMISSION AND DISTRIBUTION CO-SIMULATION AND APPLICATIONS

by

Mohammad Asif Iqbal Khan

Florida International University, 2022

Miami, Florida

Professor Sumit Paudyal, Major Professor

As the penetration of flexible loads and distributed energy resources (DERs) increases in distribution networks, demand dispatch schemes need to consider the effects of large-scale load control on distribution grid reliability. Thus, we need demand dispatch schemes that actively ensure that distribution grid operational constraints are network-admissible and still deliver valuable market services. In this context, this work develops and evaluates the performance of a new network-admissible version of the device-driven demand dispatch scheme called Packetized Energy Management (PEM). Specifically, this work develops and investigates the live grid constraint based coordinator and metrics for performance evaluation. The effects of grid measurements for a practical-sized, 2,522-bus, unbalanced distribution test feeder with a 3000 flexible kW-scale loads operating under the network-admissible PEM scheme is discussed. The results demonstrate the value of live grid measurements in managing distribution grid operational constraints while PEM is able to effectively deliver frequency regulation services.

Increased penetration of flexible loads and DERs on distribution system (DS) will lead to increased interaction of transmission and distribution (T&D) system operators to ensure reliable operation of the interconnected power grids, as well as the control actions at LV/MV grid in aggregation will have significant impact on

the transmission systems (TS). Thus, a need arises to study the coupling of the transmission and distribution (T&D) systems. Therefore, this work develops a co-simulation platform based on decoupled approach to study integrated T&D systems collectively. Additionally, the results of a decoupled method applied for solving T&D power flow co-simulation is benchmarked against the collaborator developed unified solution which proves the accuracy of the decoupled approach.

The existing approaches in the literature to study steady-state interaction of TS-DS have several shortcomings including that the existing methods exhibit scalability, solve-time and computational memory usage concerns. In this regard, this work develops comprehensive mathematical models of T&D systems for integrated power flow analysis and brings advancements from the algorithmic perspective to efficiently solve large-scale T&D circuits. Further, the models are implemented in low-cost CPU-GPU hybrid computing platform to further speed up the computational performance. The efficacy of the proposed models, solution algorithms, and their hardware implementation are demonstrated with more than 13,000 nodes using an integrated system that consists of 2383-bus Polish TS and multiple instances of medium voltage part of the IEEE 8,500-node DS. Case studies demonstrate that the proposed approach is scalable and can provide more than tenfold speed up on the solve time of very large-scale integrated T&D systems.

Overall, this work develops practically applicable and efficient demand dispatch coordinator able to integrate DERs into DS while ensuring the grid operational constraints are not violated. Additionally, the dynamics introduced in the DS with such integration that travels to TS is also studied collectively using integrated T&D co-simulation and in the final step, a mathematically comprehensive model tackles the scalability, solve-time and computational memory usage concerns for large scale integrated T&D co-simulation and applications.

TABLE OF CONTENTS

CHAPTER PAGE

LIST OF FIGURES

FIGURE PAGE

CHAPTER 1

INTRODUCTION

1.1 Motivation

Traditionally, the electric power grid is an efficient and reliable interconnected system that connects the central power generators to a low voltage (LV) Distribution System (DS) to meet consumer needs through a high voltage (HV) Transmission System (TS) at ease and minimum cost. Due to technological advancements, scarcity of resources and environmental concerns, the bulk power grid technologies are evolving towards more efficient and clean energy resources, further computerized centralized real-time monitoring and control through efficient demand management. The paragon change is realized as generating units are changing from large synchronous generators to lighter-weight generators (e.g., gas-fired turbines), and Variable Energy Resources (e.g., wind, solar, or run-of-river hydro), the TS is transforming into a greater interconnected system with DS rather than a originally designed regional system meant solely for transmission. On the distribution side as well, there is a paradigm shift in terms of rapidly increasing distributed energy resources and variable/flexible loads on the consumer side. Additionally, the technological advances on the communication sector is also adapted into power grids through increased grid control points and finer-time communication and control. These overall changes in supply and demand chain, the power system require the power grid to operate in a non-traditional way for which it is not designed and thus put under stress.

The existing grid was designed decades ago without considering this degree of variable generation & loads and the greater need of resilience & reliability. Fig. 1.1 presents the evolution of power grid to an interconnected centralized/decentralized power system with increased grid resources and increased communication and con-

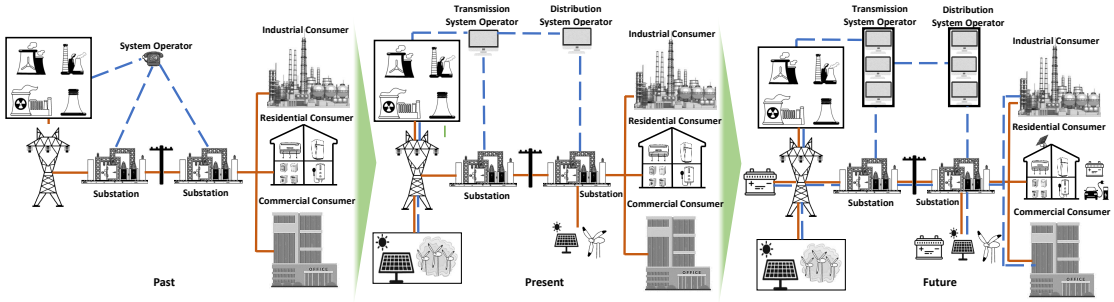

Figure 1.1: Transformation of electric grid characteristics over time

trol points. As the grid is further modernized as planned to accommodate the technical advances, the grid would be hosting variable resources at different levels through further control points and increased communication at real-time monitoring. As a whole, the grid in the future must be flexible, robust, and agile to dynamically manage network operations in real-time to balance supply and demand ensuring quality of service (QoS). The future grid is to facilitate the participation of customers as suppliers through the integration of in-house resources ensuring a solid bidirectional flow infrastructure and thus let them participate in market.

In present day, through about 3,000 distribution systems, the United state serves around 155 million customers with about 4.2 trillion kWh of energy through more than 642,000 miles of HV transmission lines, and 6.3 million miles of LV distribution lines. With the existing vastness of grid infrastructure incorporated with modernization of lifestyle creates additional dependency on electricity and thus, affordable & uninterrupted electricity is an integral part of American industry, commercial aspects, overall social life and hence, the economic growth.

The grid of the future must maintain these characteristics while meeting a number of new requirements: supporting the integration of various clean and distributed energy technologies, meeting the higher power-quality demands of modern digital

devices, and enabling consumer participation in electricity markets. Increasing the projected penetration levels of variable renewable resources, distributed generation, community energy storage, electric vehicles, and the number of active customers will require substantial changes to how the grid and its various components are designed, controlled, and protected. Therefore, an efficient, reliable, resilient, and affordable power system is an absolute must for national growth in this era of digitization. The modernization of the grid is the way to go and thus reevaluation and restructure of the operational structures is of importance and thus, detailed study and analysis is necessary on grid operations under these shifted grid characteristics.

1.2 Power Flow Analysis

Power Flow (PF) is an important tool to describe its sinusoidal steady state parameters depending on its structure and operating status, which aids in system planning, maintenance and reliable operation. Power flow analysis provides important system states such as the magnitude and angle of the voltage at each system node, slack bus power, active and reactive power generated & absorbed and line losses. The power flow solution is achieved by solving the set of non-linear algebraic equations too mainly find the either two unknown quantity of voltage magnitude (V), phase angel (δ), active power (P) and reactive power (Q) depending on the type of bus (load bus, voltage-controlled bus or slack bus).

The basic of power flow formulation follows ohm's law in a circuit and in the three-phase frame can be represented as in eqn. 5.6,

$$i = [Y][v] \tag{1.1}$$

where $[Y]$ is the network admittance, $[i]$ is the nodal current injection vector, and $[v]$ is the nodal voltage vector.

But, in practice, the power flow formulation is a set of complex non-linear algebraic equations and a fast, efficient and reliable iterative numerical algorithm is required to achieve accurate solution of the power flow. For any bus k, in a N bus power system, the power flow solution is acquired through iteratively solving the following set of equations as in eqn. 1.2 and eqn. 5.7

$$P_k = V_k \sum_{n=1}^{N} Y_{kn} V_n \ cos(\delta_k - \delta_n - \angle Y_{kn}) \tag{1.2}$$

$$Q_k = V_k \sum_{n=1}^{N} Y_{kn} V_n \ sin(\delta_k - \delta_n - \angle Y_{kn}) \tag{1.3}$$

Once the bus voltage magnitudes and their angles are computed using the load flow, the real and reactive power flow through each line can be computed. Also based on the difference between power flow in the sending and receiving ends, the losses in a particular line can also be computed. Furthermore, from the line flow we can also determine the over and under load conditions. PPF solution methods are mainly three types: Implicit Z-bus methods, Newton-type methods, and Forward-Backward sweep (FBS) methods.These methods will be discussed in detail in the next section.

Among the three important stages of the power grid, our main focus is on the Transmission and Distribution system. In this work, the transmission and distribution power flow which both are basically similar in nature except for their voltage level and impedance characteristics ($\frac{R}{X}$ ratio) serves as the core model for further development of mathematical models and case studies for analysis. PF analysis is a well researched topic in the past [Zha96, ZC97, TC02, GPC$^+$00, Ten03, BGMEA76]. Several attempts have been made to make the PF model and solution methods robust, efficient, and comprehensive [CCH$^+$91, CS95]. In the past, the power grid, especially the distribution systems were mainly passive circuits and only a few con-

trollable assets existed (e.g., voltage regulators, switches, capacitor banks) which were controlled at much slower time scale. With distribution feeders becoming active circuits and with increased penetration of controllable resources at the grid edge, several of the grid functions (e.g., voltage control, demand response, load following, frequency control) can be achieved through aggregation of the spatially distributed resources on MV/LV feeders. Some of such grid functions require efficient and comprehensive modeling of transmission and distribution grids.

The power system analysis is performed by software packages which in general are of two basic categories: commercial and research-related. The readily available and ready to use commercial packages are typically robust, well-tested and efficient. Some of the examples include PSS/E, EuroStag, Simpow, and CYME etc. But the commercial tools work like a black-box and hardly give any opportunity for modification of the models or algorithms for testing and research purposes. In addition, they are in times very expensive which makes it difficult to access for research purposes. On the other hand, for research purpose, a tool must have this flexibility for development purpose and GridLAB-D [U.] and OpenDSS [EPR] are excellent examples of such tools developed recently. However, for higher degree of flexibility in the development environment, in this work, being a matrix-oriented programming the high-level language Matlab is used to develop core power system system design, flow analysis models and plotting in each case.

In addition, as the solve time is critical for real-time performance, several efforts have been made to develop real-time simulators for power flow. OPAL-RT is an excellent platform for such application but again being a commercial software package, it is expensive and gives minimal access to its core developmental environment. For research environment, graphics processing units (GPU) are used in literature to enhance the computational efficiency as GPUs can aid in real-time power flow

solution [LLY+17] and a low-level language C/C++ can used to fully-utilize the capabilities of the GPUs.

Although, PF is a well discussed topic in the literature, however, this work mainly focuses on utilizing PF to aid aid in grid services as well as large-scale real-time simulation of Transmission and Distribution systems. The next portion of this chapter discusses the basic introduction of the research tasks tackled in this work and the motivation behind efforts in research.

1.3 Packetized Energy Management

The presence and diversity of distributed energy resources (DERs) and flexible loads such as electric vehicles (EVs), thermostatically-controlled loads (TCLs) and energy storage systems (ESSs) are rapidly growing and that changes the characteristics of the grid. If aggregated, these flexible and responsive devices can provide a significant portion of the energy and ancillary services necessary for reliable and secure operations at the consumer level to aid in intelligent demand side management [CH11, Rah08]. Coordinating demand at scale against variable whole-sale energy market requires responsive DERs which often represent large residential/commercial loads. Thus, it is valuable to guarantee that the large-scale coordination of DERs does not violate grid limits towards a more predictable and reliable grid operation.

The number, density, and diversity of behind-the-meter (BTM) distributed energy resources (DERs) and loads, such as thermostatically-controlled loads (TCLs), deferrable loads, and battery storage systems (BSS) are increasing in today's distribution systems. Via demand dispatch approaches, these connected DERs can be aggregated to provide different energy services at the bulk power level, while ensuring quality of service (QoS) for end users [CH10, Rah08]. However, existing demand

dispatch schemes often focus on coordinating devices and managing end-user device constraints and overlook the distribution grid's operational constraints. To incorporate both end-user QoS and grid constraints, one could naively construct a large (NP-hard) grid-aware device scheduling problem that embeds the distribution grid optimal power flow (OPF) problem and whose solution represents an optimal device dispatch. However, such approach generally scales poorly with the number of controllable end-points and the non-convex AC power flow constraints of large distribution networks. Furthermore, such OPF-based demand dispatch methods, which can enforce grid constraints and customers' QoS, rely on accurate and idealized network parameters and load/renewable generation forecasts, and are typically solved at minutes to sub-hourly intervals, which may not sufficiently capture the high variability on system conditions (e.g., rapid voltage fluctuations) caused by the DERs nor fast market conditions (e.g., frequency regulation).

Ensuring grid feasibility is crucial for any demand-side management (DSM) activities. In this part of the work, we incorporate grid measurements (or estimates) with a recently-developed, bottom-up coordination scheme called packetized energy management (PEM), please see [AEHH$^+$18]. The combination of sensor measurements and coordination begets a novel grid-aware implementation of PEM which is developed by collaborator in this project. Unlike many other grid-aware coordination methods, the presented approach leverages the device-driven nature of PEM and employs 'traffic-light logic' with grid measurements and constraint violations to make real-time and local decisions about devices. At its core, PEM employs internet-like packet protocols to coordinate the energy consumption of TCLs by having each device asynchronously and probabilistically request a finite-duration, fixed-power energy packet based on its local need for energy (e.g., temperature within its dead-band or its state of charge). The PEM coordinator then accepts or

denies individual energy packet requests to regulate the aggregate load based on a desired reference. If the coordinator accepts more packet requests than packets that expire, then the aggregate demand increases. Otherwise, it decreases. However, to ensure that devices can meet local energy requirements, PEM also enables devices whose energy packet requests have been denied to temporarily opt-out of the scheme and consume energy, if it needs to do so to preserve the end-user's QoS. The opted out device returns to PEM once QoS has been restored (e.g., the temperature or SoC is returned strictly within dead-band). Thus, we term PEM to be QoS-aware.

However, like in any measurement-based closed-loop voltage control of distribution feeders, the performance of 'Network-Admissible PEM' depends on the number of available measurements, frequency of the measurement update, and multi-phase measurement considerations. Note that placing sensors (e.g., μ-PMUs) on every node on the distribution circuits, and updating the measurements frequently incur high infrastructure costs and require extensive communication networks and bandwidth. Critically, this may not be necessary due to overall improvements in managing system-level constraints with a few additional grid measurements. Moreover, most of the works on voltage control with behind-the-meter assets focus on single-phase or phase decoupled circuits.

1.4 Transmission and Distribution System Co-simulation

Increasing penetration of distributed resources such as electric vehicles, storage, flexible loads in power distribution grids can provide several grid services, if aggregated, not only at the distribution level but also at the bulk transmission level. Therefore, as the modern distribution grids are designed for bi-directional power flow, the steady-state interaction of distribution system operators (DSOs) and transmission

system operators (TSO) is of utmost importance for the reliable operations of interconnected power grids [HV17, HFD$^+$17, BA17]. Moreover, as the penetration of intermittent sources in power grids is increasing, the need for solving time-series power flow at finer time resolution is increasing. This motivates us to establish computationally efficient power flow simulation tools that integrate grids at different voltage levels for real time analysis [RDM17]. Though there are some initial efforts to develop models and solve TSO-DSO power flow collectively, there is little effort towards developing models and solution algorithms that is scalable for large-scale transmission and distribution (T&D) systems and suitable for real-time performance.

The changing paradigm of power systems imposes emerging challenges for power system design, planning and operation. The paradigm shift of power systems has been reflected on modelling and simulation methods used for power system analysis as well. Simulation frameworks are urged to continuously follow growing demand for large-scale system simulation, simulation of fast system dynamics and high-fidelity models. There is a tendency toward performing joint simulation of systems that have been studied separately in the past. For instance, a joint simulation including detailed models of transmission and distribution systems is performed nowadays to analyse interdependencies and unforeseen interactions between the two systems, particularly in case of scenarios with high level of penetration of distributed generation (DG). In addition, envisioned complexity of future power systems requires simulation frameworks that enable interdisciplinary and multi-domain studies. Multi-physics simulation approach is utilised for the holistic analysis of city district energy systems that represent hybrid energy systems. Studies on architectures and concepts in smart grids require a simulation framework that enables joint analysis of power system and information and communication technology system.To maintain secure

operations of transmission and distribution systems, it is important to have a better understanding of the coupling of transmission and distribution systems.

The efficient way to examine such interactions in smart grid systems is to establish simulation process that integrates grids at different voltage levels. Hence, a need may arise to study transmission and distribution systems collectively.

Increased penetration of flexible loads and distributed resources on power distribution circuits will lead to possibility of aggregating such resources for several grid services both at the distribution and transmission levels. This will lead to increased interaction of transmission and distribution system operators, as well as the control actions at LV/MV grid in aggregation will have significant impact on the operations of bulk transmission systems. Therefore, lately, there has been some advancements to developing co-simulation platform for solving transmission and distribution (T&D) systems simultaneously for dynamic and power flow (PF) type of studies. However, the existing co-simulation platforms base mainly on decoupled approaches and a unified approach of solving T&D is largely missing in the literature.

1.5 Real-Time Analysis and Graphics Processing Unit

Power flow is an important tool to describe its steady state parameters such as the magnitude and angle of the voltage, real and reactive power, etc depending on its structure and running status which aids in system maintenance and safe operation. The changing behavior of the distribution grid summons the need to deploy a more accurate and faster PF solver that can predict the system behavior in real-time. In continuation to the aforementioned research topic, this topic would investigate the

application of a graphic processing unit (GPU)-based iterative solver in achieving a efficient real-time power flow solution for scalable networks.

The power flow solution algorithm is critical for speed up and its realization in hardware as it requires parallelizing capability to implement on GPU platforms.

Though the aforementioned works demonstrate promising results for fast power flow computation with the aid of GPUs, no work in the literature has demonstrated performance in solving power flow solutions for large-scale T&D systems using the GPU platform. This works intends to extend the ideas to solve an integrated T&D simulation in CPU-GPU platform for real-time TSO-DSO interactions.

Additionally, integrated T&D simulation has scalability concerns, and hence, a working example of large-scale integrated T&D simulation is largely missing in the literature. Since the simulation of large-scale power systems consists of solving thousands of non-linear equations, which is computationally burdensome, graphics processing units (GPU) are used in literature to enhance the computational efficiency as GPUs can overcome the limitation of LU-based direct solvers by employing parallelization [LLY+17].

1.6 Contribution

This research work develops on the works of many age-old research developments and utilizes thees well-tested methods and theories for Power Flow analysis, Packetized Energy Management, estimation of grid states, Transmission and Distribution system co-simulation, GPU based mathematical models. Nevertheless, building on these habitual theories, the following research tasks can be pointed as major contributions which are original and unique.

1.6.1 Grid-Aware Energy Management

Development of a smart network coordinator that incorporates grid measurements (or estimates) with PEM in achieving global tractability ensuring quality of service.

- Developed and mapped large-scale grid model to integrate flexible load models across the network.
- Developed comprehensive PF models to accurately acquire live grid measurements while updating the grid loading conditions upon time dependent changes.
- Leveraging the bi-directional DER coordination scheme PEM, developed a smart demand dispatch scheme that guarantees network admissible DER coordination.
- Building upon the Network-Admissible PEM [KPAew], developed practically-relevant, simulation-based analysis on the effects of the number, type, and sampling rate of grid measurement updates on the overall performance of the Network-Admissible PEM.
- Developed simulation methods evaluating the significance of intra-phase measurements on the effective voltage control of multi-phase distribution grids while considering phase-coupled unbalanced distribution grids in the Network-Admissible PEM

1.6.2 Transmission and Distribution System Co-simulation

Development of algorithms for scalable & integrated T&D simulation to analyze TD test system using decoupled and unified approach to be used for bench-marking purpose.

- Developed a comprehensive mathematical model of transmission and distribution systems for steady-state analysis. This is a significant improvement on modeling T&D over the existing efforts in the literature [HV17, SKD20, JB18, KSPK19], where the grid component models are simplified.
- Developed efficient power flow algorithms that can effectively handle integrated transmission and distribution circuits. The developed algorithm scales up very well for large-scale integrated T&D systems and exhibits superior computational performance.

1.6.3 GPU based T&D System Co-simulation

Implemented the large-scale power flow model for Transmission System (TS)- Distribution System (DS) interaction in a low-cost CPU-GPU hybrid computing platform, to demonstrate the speed up, and to compare the solution speed with respect to the existing real-time tools. To the best of our knowledge, this will be the first work to implement large-scale scalable T&D simulation in GPU platform compared to the existing literature [LLY$^+$17, HGS17, RTO17], which focused on transmission systems and [ADK12] on distribution system only, and provide a low-cost solution compared to the expensive off-the-shelf commercial tools available for integrated T&D power flow [JB18].

1.7 Summary

The paradigm shift of the distribution grid with the heavy penetration of DERs and flexible loads such as electric vehicles (EVs), TCLs such as water heaters, fridges, kitchen appliances, and energy storage systems (ESSs) changes the overall characteristics of the DS through additional load (EVs/battery) and newly bidirectional

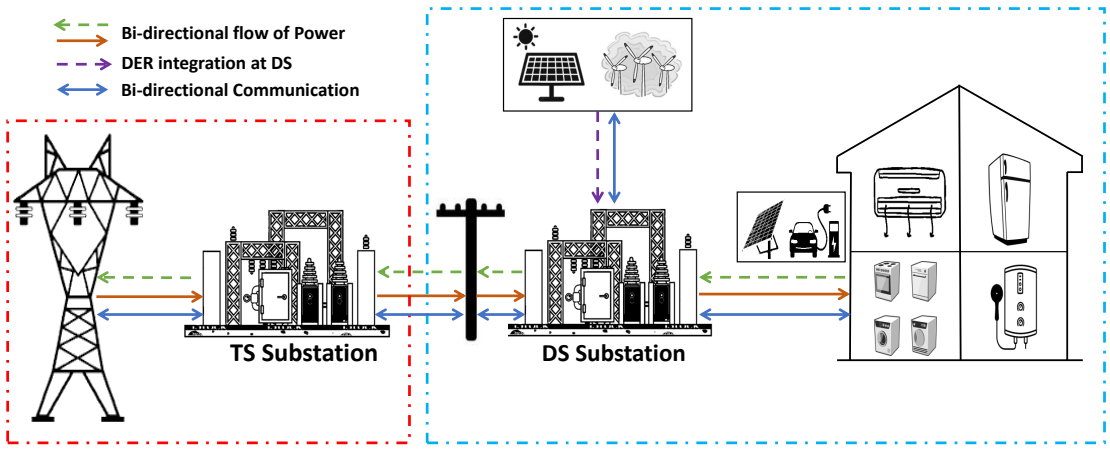

Figure 1.2: Transformation of distribution grid and increased interaction with transmission grid

flow of power. Under this current strategy and future developments, the customers are becoming suppliers by selling their additional resources back to grid and hence, the distribution grid becomes active from a passive network with flow of power in the direction of the transmission network by creating a bidirectional power flow system with increasing communication needs within the operators. While the research work on grid-aware Packetized Energy Management investigates the network constraints and develops a smart coordinator to handle such additional penetration of new loads and bidirectional power flow through demand management, it is also important to look into the characteristic evolution of the transmission network as well.

Fig. 1.2 provides a clear idea on the the active future grid where the residential consumers in addition to traditional loads, now hosts flexible loads, EV and PV sources which have the capability to sell power back to the grid after satisfying consumer needs that travels all way to the main transmission grid. The distribution block on the right side in Fig. 1.2 the residential consumer holds varieties of modernized devices which leads to increased interaction in terms of both energy flow and communication compared to the present or past grid scenario as presented

in Fig. 1.1. In addition to that, the grid is now hosting DERs connected to the distribution grid and these all have changed the unidirectional flow of power to a bidirectional flow and changed the way DS communicates with TS block on the left side of Fig. 1.2.

In such distribution system with highly variable generation, unconventional dynamics due to interactions among multiple inverters and bidirectional flow of energy will lead to increased interaction between transmission and distribution systems which needs to be investigated. An efficient way to examine such interactions in smart grid systems is to establish a simulation process that integrates transmission and distribution grids at different voltage levels to study the integrated systems collectively for secure and reliable operations of interconnected power grid.

Therefore, the research task on the Transmission and Distribution (T&D) System Co-simulation takes up on the challenge to develop a decoupled approach for solving integrated T&D system and efficiently benchmarks it with the collaborator developed unified solver for accuracy.

With this increasing variable behavior of the distribution grid with the transmission grid, the nature and communication time frame also shifts towards finer time resolution in real-time. Additionally, there is research gap in the current literature in simulating large-scale integrated T&D systems as with increasing system size, the computational burden increases. This motivates the development of a computationally efficient and scalably generic simulation framework that integrates grids at different voltage levels, enabling time-series power flow simulation of integrated T&D systems for real time analysis. Hence, in the third task, using a CPU-GPU hybrid platform , an efficient and fast PF solver is developed with the intent to solve large-scale power flow model using a comprehensive mathematical model of transmission and distribution systems for steady-state analysis.

1.8 Organization of the Dissertation

1.8.1 Chapter 2: Background and Literature Review

A detail overview of the basic mathematical models of the well-established power flow methods and simulations are discussed in this chapter. The discussion includes the present-day research efforts and publications to analyze the advances and advancements in this dissertation topic. This chapter also evaluates the research gaps and opportunity for further developments and hence, justifies the research efforts made in this work.

1.8.2 Chapter 3: Network Admissible PEM

This chapter provides preliminaries on PEM including the device and coordinator level PEM logic. Network admissible PEM is built on the accuracy of power flow solver and live grid measurement. So, the overall approach including the PF solver, acquisition of grid measurements and the significance of intra-phase measurements on the effective voltage control of multi-phase distribution grids is discussed here to explain the algorithmic approach of the Network-Admissible PEM. Several evaluation metrics are adopted to analyze the performance of the Network-Admissible PEM. Next, the developed case studies are presented and numerical simulation results are presented and discussed using the developed evaluation metrics in concluding the task.

1.8.3 Chapter 4: T&D Co-simulation

One of the major challenge in T&D Co-simulation is the choice of right mathematical model for the simulation. Here, at first, the simulation methods, i,e the PF solvers

are discussed and the suitability of the solver for integrated T&D Co-simulation. Then, the mathematical modeling of the decoupled and unified approach including the comprehensive grid model is discussed. In the next section, the developed case studies are presented and the acquired results are bench-marked for accuracy of the developed numerical models.

1.8.4 Chapter 5: GPU-based T&D Co-simulation

Developing on the integrated T&D Co-simulation, this chapter discuss the suitable common power flow solution methods for the decoupled and unified approach for solving large-scale integrated TD systems at a faster time frame. GPU is used here as a computational tool to acquire PF as a faster time frame. Then, a basic overview of GPU and the GPU language environment is discussed briefly. In the next part, the numerical simulation models and the performance evaluation metrics are discussed. Next section discusses the case studies, acquired results and evaluates using the metrics to make concluding remarks.

1.8.5 Chapter 6: Conclusion and Future Work

This chapter signifies major findings of each research task and presents research tasks for the future. This includes the limitation of specific solver in simulating specific test system and the work-around.

CHAPTER 2

LITERATURE REVIEW

2.1 Introduction

In this chapter, the well established power flow solver and the use of these solvers along with the research focus related to recent developments in the literature is discussed. The basic introduction of power flow solvers and the usage of these solvers in the literature is discussed in the Section 2.2. Section 2.3 discusses the relevant literature related to packetized energy management and grid-awareness in addition to grid states. Section 2.4 would present the co-simulation advancement and limitations of T&D co-simulation till date. Section 2.5 discusses the limitation of large-scale T&D co-simulation in real-time while presenting the recent advancements.

2.2 Power Flow Solvers

The power flow and the selection of an applicable method to solve power flow is the most basic prerequisite for analyzing secure steady state and optimal operational setting of the present day grid and future planning and design. The methods of power flow analysis can be divided into two major categories; namely, deterministic and probabilistic methods, where the later basically deals with the system uncertainties and the method includes the uncertainties in terms of probability density function to solve the system states. Our research works focus on the deterministic methods which again can be divided into three main categories such as direct iterative method, Gauss-type methods and Newton-type methods which all uses the network provides static data including generation, connected loads and calculate the power flow in achieving the static grid state using the given grid configuration.

A great application of the first category is the the forward/backward sweep (FBS) methods which is mostly suitable for the distribution systems. FBS methods exploit the radial or weakly meshed topology of distribution systems and are based on ladder circuit analysis [KM76, Ker84, CS95]. FBS method is preferred for distribution system PF due to its simplicity in multi-phase environment and faster speed. Though FBS generally takes more iterations than NR, it requires less memory and less computation complexity on each iteration as it does not need to store and invert full Y-bus or Jacobian matrices [MGP16]. Several variants of FBS have been proposed to make the model more efficient [CCW07, GD99] and incorporate voltage controlled buses [ZT02, JWZS14]. FBS is shown as a robust approach for solving distribution grid power flow and its convergence is less dependent on R/X ratio of the feeders; even in large-scale applications [BCCN00, CFO03].

In the second category, most appropriate representative of Gauss-type methods are Gauss-Seidel and the Implicit Z-bus Gauss method. In this research Implicit Z-bus methods are used which is a Gauss bi-factored Y-matrix (GBY) method and is derivative free, and hence, simple to implement [LSCT99, CCH$^+$91]. Implicit Z-bus methods involve the solution of a linear set of equations for constant current injections and an iterative method for constant power loads. Recently, in [BG18b], sufficient conditions for the convergence of Implicit Z-bus method are derived for ZIP loads. However, its convergence could be slower and shown to diverge for distribution systems with voltage controlled buses [CZDK14].

The third category i.e. the Newton-type methods such as Newton-Raphson (NR) method and its variants are common in solving transmission level power flow problems [TH67]. Due to radial or weakly meshed structure, and high R/X ratio, Newton-type methods traditionally was not preferred for Distribution system PF in the past [BG18b, CCH$^+$91] and even authors mentioned that NR could fail for

specific distribution systems [GD99]. However, Newton-type methods are shown to be successful in solving power flow for both transmission and distribution system and generally require less number of iterations to converge [SMP+18, KSS08]. However, each iteration of NR requires updating elements of Jacobian and inverting the Jacobian matrix, which are computationally involving steps. NR method applied to current injection based formulation, as in [GPC+00], requires only a few of the Jacobian elements to be updated in the iteration; hence, this approach is faster compared to NR method applied to power injection based formulation. [PAP+04] introduced a robust four-wire current injection based NR method including neutral wires and ground impedance in solving unbalanced three-phase PF. To achieve computational efficiency, a fast decoupled version of DPF is developed in [ZC95], but this approach is not the extension of the fast decoupled method for solving transmission level power flow which exploits the low R/X ratio of transmission lines [SA74]. Several attempts were made to improve performance of the fast decoupled method with high R/X ratio including the empirical adjustment made in the Jacobian matrix [RB88]. NR method can be readily applied to solve the transmission and distribution system under unsymmetrical conditions to solve power quality problems [LN97]. NR method have higher reliability in terms of robustness and higher rate of convergence under suitable choice of initial starting conditions specially when scalable systems are under investigation [MKG+07].

Overall, NR method has the robustness and scalability required to solve a complex power system that hosts a combination of all types of network buses and hence NR methods or it;s variant is preferred to solve both transmission and distribution system in the literature extensively and in this work.

2.3 Network Admissible Packetized Energy Management[1]

Ensuring grid feasibility is crucial for any demand-side management (DSM) activities. In this context, the authors in [LM19] proposed congestion and voltage profile management by estimating the expected network profiles (voltage, power flow, etc.) and energy usage variations. To ensure grid feasibility of diverse DERs, the work in [CDZL20] uses multi-period optimization models to aggregate the active power flexibility by approximating the exact feasible region of the net power injection at the substation level with an inner-box region. In [MR19], authors propose node-wise computation of power injection and withdrawal limits using OPF-based models. Disaggregating the net flexibility as obtained in [CDZL20] to nodal level or estimating the nodal injection bounds that ensures grid feasibility could still render challenging optimization problems [WBP+19]. Therefore, in [NA19a, NA19b], the authors developed a provable convex inner approximation of the feasible region that is able to disaggregate dispatch signals to nodal level that do not violate the grid constraints. Realising the uncertainty of incoming usage request of connected flexible loads, in [LBT+19] the authors developed a control formulation for handling plug-and-play charging requests of flexible loads in a distribution system and ensured grid feasibility through a convex formulation of the distribution grid model [FL13]. The grid feasibility can also be ensured through the estimation of DER and flexible load hosting capacity as in [WCGW16, JMW16]. In [BBDZ18, SAM19], the grid feasibility is ensured through the design of local droop settings to control active/reactive power of DERs.

Given the high computational needs, the optimization based models are intended to provide bounds at coarse time scale (sub-hourly) that may not capture high

[1]A portion of Section 2.3 discussing literature review on PEM is contributed by our research collaborator team of University of Vermont led by Dr. Mads R. Almassalkhi.

variability on grid conditions due to intermittency of DERs. To ensure robustness in managing the grid constraints, particularly for forecasting uncertainties and high variabilities of DERs, the coarse time-step, optimization-based methods can be complemented by feedback obtained from the grid measurements/state estimators [GZZ+20, PBD20]. That is, as the deployment of low-cost sensors at the grid-edge intensifies and are combined with existing real-time automatic controllers (RTAC) and micro-phasor measurement units (μ-PMU), it opens up new data-driven applications for feedback-based coordination of DERs in power distribution networks that respects constraints and network limits [RAW21].

In this task, we incorporate grid measurements (or estimates) with a recently-developed, bottom-up coordination scheme called packetized energy management (PEM), please see [AEHH+18]. The combination of sensor measurements and coordination begets a novel grid-aware implementation of PEM. Unlike many other grid-aware coordination methods, the presented approach leverages the device-driven nature of PEM and employs 'traffic-light logic' with grid measurements and constraint violations to make real-time and local decisions about devices.

However, like in any measurement-based closed-loop voltage control of distribution feeders, the performance of 'Network-Admissible PEM' depends on the number of available measurements, the frequency of the measurement update, and multi-phase measurement considerations. Note that placing sensors (e.g., μ-PMUs) on every node on the distribution circuits and updating the measurements frequently incur high infrastructure costs and require extensive communication networks and bandwidth. Critically, this may not be necessary due to overall improvements in managing system-level constraints with a few additional grid measurements. Moreover, most of the works on voltage control with behind-the-meter assets focus on single-phase or phase decoupled circuits. Removal of mutual impedance

from distribution circuits causes significant voltage error in the phase-decoupled models [ISPK21]. Specifically, the intra-phase dependency is not straightforward as active voltage control in one phase can worsen the voltage profiles on other phases [KZGB16]; hence, it necessities full three-phase voltage measurements for effective control of unbalanced distribution feeders.

2.4 Transmission and Distribution System Co-simulation

The convergence of unified T&D is challenging due to different $\frac{R}{X}$ ratios of transmission and distribution systems and lack of a single scalable method to solve the power flow of the unified system. Therefore, T&D model and solution methods in literature follow decoupled approaches [HV17], where transmission and distribution systems are decoupled at interface buses and solved independently (employing specialized algorithms) either sequentially or simultaneously depending on the capability of the computing machines. In the modeling, the Transmission Systems (TS) are modeled based on positive-sequence or three-sequence while the Distribution Systems (DS) are based on three-phase modeling. These approaches use existing off-the-shelf tools in solving respective transmission and distribution models [KSPK19].

In conventional simulation tools, transmission and distribution circuits are treated as separate systems and are analyzed independently. In such tools, distribution systems are represented by lumped loads while solving the transmission system. On the other hand, the transmission system is represented using a constant voltage source while solving distribution circuits [JB18]. Although, the existing electromagnetic transient (EMT) simulators can solve integrated transmission and distribution systems, the simulation procedure may not be scalable for large-scale systems due to inherent computational burden. Moreover, EMT level simulation may not be

necessary for the entire power grid if power flow analysis, stability analysis or dynamic studies are the focus. Therefore, in order to reduce computational burden of EMT simulations, efforts have made in the past to develop co-simulation platforms that can combine EMT simulation and transient stability analysis (TSA) tools together such that the detailed EMT type of studies are carried out only for high frequency switching devices [JDS$^+$09, ZGW$^+$13, TGK19]. Similarly, in [PAGV14], a co-simulation platform is built that can interface phasor-based and EMT simulators. Lately, efforts have made to built co-simulation platforms to solve Transmission and Distribution Systems (T&D) directly in phasor domain for several applications (power flow [SGZ$^+$15, HV17], dynamic simulation [SGZ$^+$15], contingency analysis [LWSG15], etc.)

Existing T&D co-simulation methods follow decoupled approaches, where transmission and distribution systems are decoupled at interface buses. Most of the methods use off-the-shelf simulators for solving transmission and distribution systems separately, and user-built interfaces are used for data exchange between the simulators. A unified approach for simultaneously solving T&D models are discussed in [MT09] (for power flow) and [JPB$^+$16] (for dynamic simulation). In [SGZ$^+$15], a global power flow analysis based on master–slave splitting of T&D system is used. Convergence of the method is demonstrated; however, it is not known if the power flow solution of T&D using decoupled approach would converge to the true solution compared to a unified approach as in [MT09]. In[HFD$^+$17], an open-source framework, 'framework for network co-simulation' (FNCS), is developed for T&D co-simulation, where FNCS is used as the information interface, GridPACK as transmission system simulator, and GridLAB-D as distribution system simulator. In [HV17], a Diakoptics based simulation approach for T&D co-simulation (both power flow and dynamic simulation) are built. In the modeling, the transmission system is

based on three-sequence modeling and distribution system is based on three-phase modeling. The authors argued that the analysis in mixed frame of reference allows use of existing mature methodology/tools in solving respective transmission and distribution models.

In [JB18], a very large T&D system (100,000+ nodes) is solved using commercial ePHASORSIM solver, and a real-time performance was achieved exploiting the parallel processing. Decoupled approaches, as in [JB18, AVC15, HV17, MT09], exhibit benefits that the algorithms can be parallelized. However, inappropriate choice of simulation time step and inherent time delays on the decoupled approach may lead to divergence of the solution [VKA18]. Moreover, solutions obtained from phasor-based decoupled approaches needs to benchmarked against phasor-based unified T&D co-simulation approaches [MT09, JPB+16]. Since the benchmarking solutions to T&D co-simulation are not available, efforts have made in the past to compare against solutions obtained from the EMT solvers (and by using Fourier filters) [HV17].

Existing decoupled approaches take the advantage of using off-the-shelf simulators to solve the integrated T&D systems through proper information exchange with reduced computational burden. In all the aforementioned decoupled approaches, one major missing component is the absence of an appropriate benchmark to validate the results as there exists no standard T&D test results based on unified co-simulation approach in phasor domain. Therefore, one of the objectives of this work is to develop a unified T&D test system that can serve as a benchmark for decoupled approaches.

2.5 Real-time Co-simulation on GPU

The power flow solution algorithm is critical for speed up and its realization in hardware as it requires parallelizing capability to implement on GPU platforms. Forward-Backward algorithm shows promising results with possibility of parallelizing for radial feeders [ADK12]. Newton-Raphson (NR) based method shows greater speed-up in GPU compared to other methods for transmission system, while the absolute solve time of NR-based method still would be slow as system size grows [GJY+12]. It is shown in [XFC13], using multi-frontal method that the efficiency of solving sparse linear equations of NR method can be improved by using GPU based linear algebra library. GPUs parallel programming library coupled with efficient power flow solving algorithm has found to provide real time analysis of large-scale power systems and at least two orders of magnitude faster than the CPU counterpart [WCK+19, ZBC+18].

As the solve time is critical for real time performance, the development of computationally efficient models and methods are crucial to simulate large-scale integrated T&D systems. Additionally, integrated T&D simulation has scalability concerns, and hence, a working example of large-scale integrated T&D simulation is largely missing in the literature. Since the simulation of large-scale power systems consists of solving thousands of non-linear equations, which is computationally burdensome, graphics processing units (GPU) are used in literature to enhance the computational efficiency as GPUs can overcome the limitation of LU-based direct solvers by employing parallelization [LLY+17]. By exploiting the sparse vector/matrix operations, the massively parallel architecture of GPUs are utilized in a hybrid GPU–central processing unit (CPU) computing environment in [HGS17, RTO17] to further reduce the solve time. GPU can aid in achieving additional layer of parallelism with better

coalesced memory accesses in solving massive number of tasks in achieving higher speed up in simulation compared to traditional platforms [ZFB+17, ZBC+17]. Additionally, use of pre-conditioner have been found effective for a GPU based platform [LL15]. Heterogeneous CPU-GPU hybrid platform with generalized minimum residual (GMRES), bi-conjugate gradient based sequential, and parallelly iterative power flow solver can provide better parallelism, simulation efficiency and convergence as demonstrated in [LWT13, Gar10].

An off-the-shelf commercial tool has demonstrated large-scale T&D simulation [JB18]; however, the method is proprietary and requires dedicated hardware. The work in the literature lacks comprehensive component modeling (particularly on the distribution side), scalability, and real-time performance of large-scale T&D systems for steady-state interactions in TSO-DSO. Though the aforementioned works demonstrate promising results for fast power flow computation with the aid of GPUs, no work in the literature has demonstrated performance in solving power flow solutions for large-scale T&D systems using the GPU platform. This works intends to extend the ideas to solve an integrated T&D simulation in CPU-GPU platform for real-time TSO-DSO interactions.

Another challenge in solving integrated T&D power flow is the lack of a single algorithm that can be readily applied to transmission and distribution systems. Though Newton-Raphson (NR)-based algorithms are used in solving transmission and distribution systems, it lacks the required computational performance for large-scale systems as the Jacobian matrix needs to be computed and inverted every iteration of NR. On the other hand, decoupled power flow methods can overcome the issues of NR methods; however, the methods fail for distribution systems. Similarly, the distribution system-specific power flow methods such as backward-forward sweep (BFS) and Z-bus (implicit) methods cannot be extended to transmission level

studies. Therefore, with the focus on the limitations of the existing works and solution algorithms for integrated T&D simulation, this work proposes to contribute as follows.

- To develop a comprehensive mathematical model of transmission and distribution systems for steady-state analysis. This will be a significant improvement on modeling T&D over the existing efforts in the literature [HV17, SKD20, JB18, KSPK19], where the grid component models are simplified.
- To develop efficient power flow algorithms that can effectively handle integrated transmission and distribution circuits. The proposed solution algorithm on transmission side, which will be a variant of inexact NR, does not require inversion of the Jacobian matrix every iteration and hence scales up very well for large-scale integrated T&D systems and exhibits superior computational performance.
- To implement the large-scale power flow model for TSO-DSO interaction in a low-cost CPU-GPU hybrid computing platform, to demonstrate the speed up, and to compare the solution speed with respect to the existing real-time tools. To the best of our knowledge, this will be the first work to implement large-scale scalable T&D simulation in GPU platform compared to the existing literature [LLY+17, HGS17, RTO17], which focused on transmission systems and [ADK12] on distribution system only, and provide a low-cost solution compared to the expensive off-the-shelf commercial tools available for integrated T&D power flow [JB18].

2.6 Summary

This chapter hereby presented the applicability of mathematical methods in power flow analysis and coherently discusses the research development is all of the research projects of this dissertation in identifying the need and the research gap while mentioning the major contribution of these tasks.

CHAPTER 3

NETWORK-ADMISSIBLE PACKETIZED ENERGY MANAGEMENT

3.1 Introduction

In this chapter the major development of the network -admissible PEM method and the coordinator decision making process is discussed along with the development of the grid constraints. Section 3.2 provides a basic overview of preliminaries on PEM. Section 3.3 provides algorithmic description on the Network-Admissible PEM. Section 3.4 discusses performance evaluation of Network-Admissible PEM using unbalanced distribution system. Section 3.5 provides a summary of the research findings.

3.2 Packetized energy management preliminaries

This section provides a summary of grid-agnostic PEM control logic at the device and coordinator layers.[1]

3.2.1 Device Level PEM Logic

Consider device n with measured or estimated energy state over discrete time interval k of duration Δt, $x_n[k]$. This device is endowed with local control logic that relates the $x_n[k]$, its user-defined set-point x_n^{set}, and its comfort range, $[\underline{x}_n, \overline{x}_n]$, to a probability of making a request for a finite-duration, fixed-power energy packet to

[1]The overall PEM preliminaries (Section. 3.2) is developed by our research collaborator team of University of Vermont led by Dr. Mads R. Almassalkhi. We have developed the demand dispatch scheme in presence of grid constraints and efficiently integrated with PEM scheme to study the impact on the overall distribution grid.

the coordinator (e.g., 5-minute, 4 kW or 0.33 kWh energy packet request). As an example, the probability that device n makes a request during interval Δt is illustrated in Fig. 3.1 via the following relation for a charging (i.e., power consumption) packet:

$$P_{\text{req}}(k) := 1 - e^{-m_R \mu_n(x_n[k])\Delta t} \tag{3.1}$$

where m_R is the mean time-to-request (MTTR) when $x_n[k] = x_n^{\text{set}}$ and $\mu_n(x_n[k]) \geq 0$ is a state-dependent rate parameter given by,

$$\mu_n(x_n[k]) := \begin{cases} \frac{\overline{x}_n - x_n[k]}{x_n[k] - \underline{x}_n} \cdot \frac{x_n^{\text{set}} - \underline{x}_n}{\overline{x}_n - x_n^{\text{set}}} & \text{if } x_n[k] \in (\underline{x}_n, \overline{x}_n) \\ 0 & \text{if } x_n[k] \geq \overline{x}_n \end{cases} . \tag{3.2}$$

Discharging (i.e., power injection) packet request logic can be defined similarly and is also illustrated in Fig. 3.1. Thus, for a given local dynamic energy state (or a device's need for energy), the probability of making a request is defined. This probability is compared with an independent sample from uniform distribution to determine if a request is made from device n at time-step k.

If the request is made and accepted by the coordinator, the device switches from standby to a constant-power charging/discharging (consumes/supplies energy) state at the device's rated power level $\pm P_n^{\text{rate}}$. The constant power level is maintained for the duration of the packet length when the packet then *expires*, unless the packet is *interrupted* prematurely (to avoid exceeding the comfort range).

In addition, if a device's requests are repeatedly denied by the coordinator, the device's energy state may exceed its comfort range. Owing to the QoS-aware design of PEM, the device will then notify the coordinator that it is automatically *opting out* of PEM and will consume/supply the necessary energy to return the energy state to within its defined comfort range upon which the device updates the coordinator that it has returned to PEM mode. The use of packet-based (net)

consumption and event-based device communications represents a novel, scalable approach for a centralized coordinator to estimate the aggregate demand without real-time power measurements from the entire fleet. Next, we define how packet requests are managed by the PEM coordinator to dynamically regulate aggregate (net) demand.

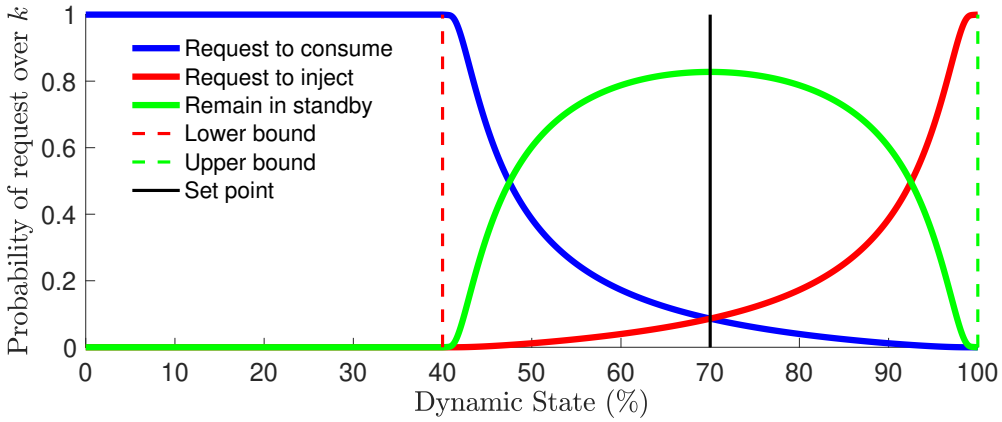

Figure 3.1: Probability of a bidirectional device (e.g., ESS) requesting to the coordinator to either consume power (blue) or inject power (red) over a discrete-time interval k. If neither or both request types are made, then the device remains in standby (green). Clearly, for an electric water heater, there is no option to inject power, so device's packet request logic simplifies.

3.2.2 Coordinator Level PEM Logic

Due the asynchronous implementation of PEM, an energy packet request from any device can arrive at the coordinator at any time. This implies that over a sufficiently small time interval (e.g, 10ms, which can be different from device's interval Δt), it is reasonable to assume that the coordinator only receives a single device event. The event could be an incoming charging/discharging packet request, $u_{\mathrm{c/d},n}[k] \in \{0, 1\}$, which is either accepted or rejected (i.e., $y_{\mathrm{c/d},n}[k] \in \{0, 1\}$ with $y_{\mathrm{c/d},n}[k] \leq u_{\mathrm{c/d},n}[k]$). Besides packet requests, the coordinator can also receive event types related to

previously accepted packets expiring ($y^{\text{exp}}_{\text{c/d},n}[k] = 1$) or being interrupted ($y^{\text{int}}_{\text{c/d},n}[k] = 1$) and devices opting out ($y^{\text{opt}}_{\text{c/d},n}[k] = 1$). From the incoming stream of events, the coordinator can then construct an online estimate of the aggregate demand. For example, for a fleet of switch loads (i.e., with only charging packets and $P^{\text{rate}}_n > 0$), the aggregate demand at time-step k can be estimated as:

$$P_{\text{agg}}[k+1] := P_{\text{agg}}[k] + \sum_{n=1}^{N} P^{\text{rate}}_n \Delta y_{\text{c},n}[k], \tag{3.3}$$

where, $\Delta y_{\text{c},n}[k] := y_{\text{c},n}[k] - y^{\text{exp}}_{\text{c},n}[k] - y^{\text{int}}_{\text{c},n}[k] + y^{\text{opt}}_{\text{c},n}[k]$ and we assume that the time-step k is sufficiently small such that no more than a single device event takes place across the fleet (i.e., $\sum_{n=1}^{N} y_{\text{c},n}[k] + y^{\text{exp}}_{\text{c},n}[k] + y^{\text{int}}_{\text{c},n}[k] + y^{\text{opt}}_{\text{c},n}[k] \leq 1$ for all k). Clearly, the aggregate demand increases when packets are accepted or devices opt out and demand decreases when a packet expires or is interrupted. Note that the coordinator's only decision is whether to accept or reject a packet request (i.e., determine $y_{\text{c/d},n}[k]$), which is based on the difference between $P_{\text{agg}}[k]$ and a desired target reference power $P_{\text{ref}}[k]$.

This gives rise to the coordinator's control policy, whose objective is to minimize the tracking error $e[k] := P_{\text{ref}}[k] - P_{\text{agg}}[k]$ and is defined as follows for a fleet of switch loads:

$$y_{\text{c},n}[k] := \begin{cases} 1, & \text{if } u_{\text{c},n}[k] = 1 \ \wedge \ e[k] \geq P^{\text{rate}}_n/2 \\ 0, & \text{else} \end{cases}. \tag{3.4}$$

Generalizing the above to the case of coordinating a fleet with both charging and discharging requests is straightforward. For further details on modeling and control of a fleet under PEM, please see prior works [AEHH$^+$18, DA20, BKOA21]. Note that the coordinator's control policy is similar to a relay controller that accepts a packet when the tracking error is above a threshold ("green light") and reject otherwise ("red light"). However, unlike traditional relay control from a single plant, the

coordinator responds to asynchronous, stochastic requests from N plants, which permits accurate tracking.

The key contribution in this manuscript is to extend the coordinator's control policy in (3.4) to incorporate and understand the effect of distribution grid measurements into the packet acceptance/rejection logic. These measurements enable PEM to be cognizant of the network's nodal voltage and transformer apparent power limits and only accept packet request if they reduce tracking error **and** do not exacerbate any network violations, which gives rise to a *Network-Admissible PEM* and is described next.

3.3 Network-Admissible PEM

3.3.1 Overall Approach

The overall Network-Admissible PEM approach is illustrated in Fig. 3.2, where the PEM coordinator as in [AEHH$^+$18, AFH17] is integrated with a (grid) Constraint Coordinator. In regular PEM scheme, energy packet requests are made by the devices to the PEM coordinator, which are accepted or rejected by the coordinator in real time to track desired reference setpoints (as explained in Section II). The accepted requests are handled by the Constraint Coordinator in the next step, which checks the grid constraints based on live grid measurements to generate traffic-like logic to determine, in real time, whether packets requests are network admissible. The details of Network-Admissible PEM is provided in [KPAew].

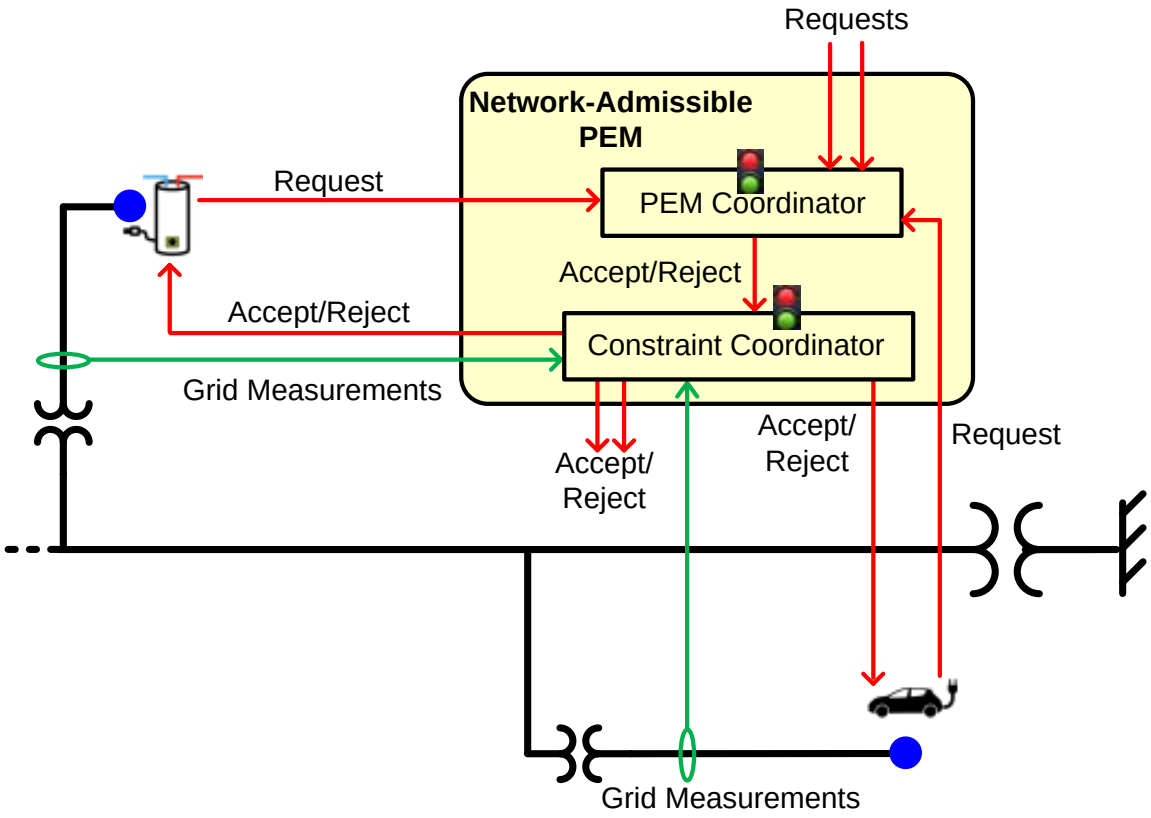

Figure 3.2: Network-Admissible PEM-based demand dispatch scheme.

3.3.2 Multi-Phase Measurement Considerations

The local voltage control schemes in literature use voltage measurements only from the controlled node. Refer to Fig. 3.3, where a local controller at node i_a (which is phase-a of three-phase bus i) takes the voltage measurements only from the same node, i.e., V_{i_a}, while the voltage measurements of other two phases of the same bus, i.e., V_{i_b} and V_{i_c} are not used. Such voltage control schemes are applied to three-phase unbalanced feeders with strong assumption that improvement in voltage performance on one phase of a multi-phase bus does not worsen the voltage profile of other phases of the same bus. The assumption would be that a load of I_{i_a} causes voltage drop on all three phases of the bus i with respect to bus j, i.e., $|V_{i_a}| \leq |V_{j_a}|$,

$|V_{i_b}| \leq |V_{j_b}|$, and $|V_{i_c}| \leq |V_{j_c}|$. However, a closer look at voltage drop model in three-phase circuit suggests that the mutual coupling among phases may impact the voltages of other phases differently. The voltages on two ends (bus j and i) of three-phase distribution feeder with a load of I_{i_a} can be modelled as,

$$\begin{bmatrix} V_{i_a} \\ V_{i_b} \\ V_{i_c} \end{bmatrix} = \begin{bmatrix} V_{j_a} \\ V_{j_b} \\ V_{j_c} \end{bmatrix} - \begin{bmatrix} Z_{aa} & Z_{ab} & Z_{ac} \\ Z_{ab} & Z_{bb} & Z_{bc} \\ Z_{ac} & Z_{bc} & Z_{cc} \end{bmatrix} \begin{bmatrix} I_{i_a} \\ 0 \\ 0 \end{bmatrix}. \tag{3.5}$$

The phasor diagram in Fig. 3.3 shows that the load of I_{i_a} can lead to voltage rise on node i_b (with respect to node j_b), i.e., $|V_{i_b}| \geq |V_{j_b}|$ due to mutual coupling of the phases. We can arrive at similar observations if loads are connected at nodes i_b or i_c. This clearly indicates that a local control scheme that improves voltage on one phase can negatively impact the voltages on other phases of the same bus. Therefore, for any measurement based control approach, voltage measurements of other phases of the same bus is required for effective voltage management of a

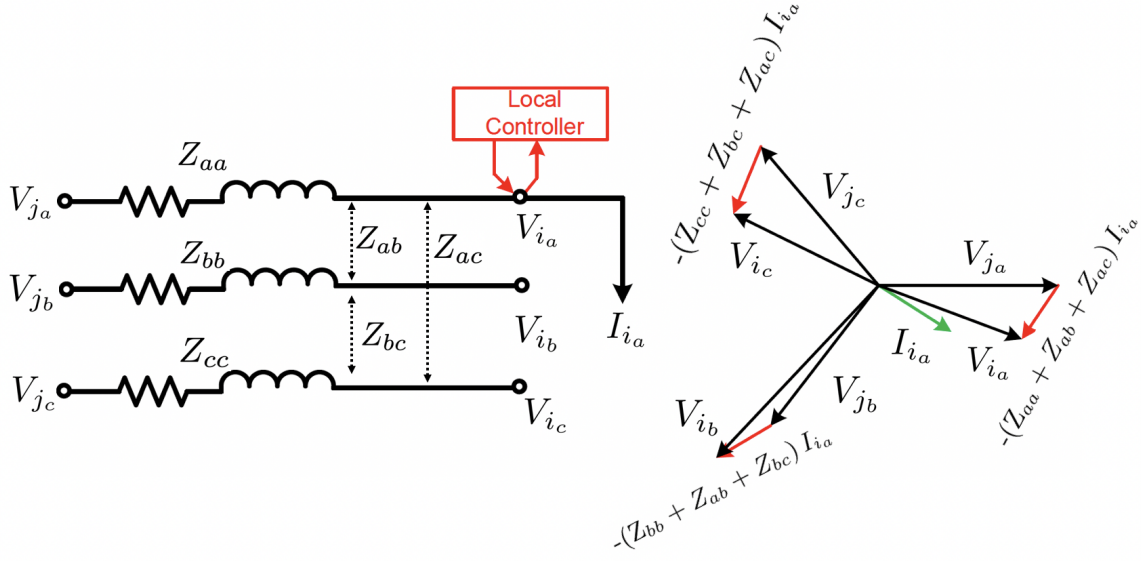

Figure 3.3: Equivalent circuit and voltage drop model of three-phase unbalanced distribution feeder.

single phase node. Therefore, in the proposed Network-Admissible PEM scheme, we consider intra-phase measurements in the Constraint Coordinator (see Fig. 3.2).

3.3.3 Network-Admissible PEM Algorithm

Consider i_p represents index for a single phase node at bus i, i_{p+} represents all phases of the same bus where node i is connected to, and $M[i_p] \in \{0, 1\}$ is a parameter that represents if voltage at node i_p is measured or not. $\underline{V[i_p]}$ and $\overline{V[i_p]}$ are the prescribed minimum and maximum voltage magnitude bounds. Based on the overall approach shown in Fig. 3.2 and the multi-phase voltage measurement consideration as described earlier, we build the proposed Network-Admissible PEM algorithm as shown in Algorithm 1. Note that Algorithm 1 is provided with respect to charging packet requests only; however, similar logic can be readily developed for discharging packet request in the Network-Admissible PEM.

: Network-Admissible PEM [1]

Incoming Packet Request $u_{\mathrm{c},n}[i_p, k]$ $\neg(u_{\mathrm{c},n}[k] = 1 \ \wedge \ e[k] \geq P_n^{\mathrm{rate}}/2)$ Refer to (4). Reject Packet: $y_{\mathrm{c},n}[i_p, k]$=0. Grid Constraint Management. $M[i_p] = 1$ Node i_p is measured. $\underline{V[i_{p+}]} \leq \left|V[i_{p+}, k]\right| \leq \overline{V[i_{p+}]}$ Accept Packet: $y_{\mathrm{c},n}[i_p, k]$=1. Voltage violation. Reject Packet: $y_{\mathrm{c},n}[i_p, k]$=0. Accept Packet: $y_{\mathrm{c},n}[i_p, k]$=1.

3.4 Numerical Simulation

In this section, we study the impact of varying PEM packet length (P_t) and grid voltage measurement update rate (S_t) on the Network-Admissible PEM scheme. We also evaluate the performance of Network-Admissible PEM scheme with single-phase versus multi-phase voltage measurements. Additionally, we study the impact

of the number of voltage measurements on the performance of Network-Admissible PEM scheme.

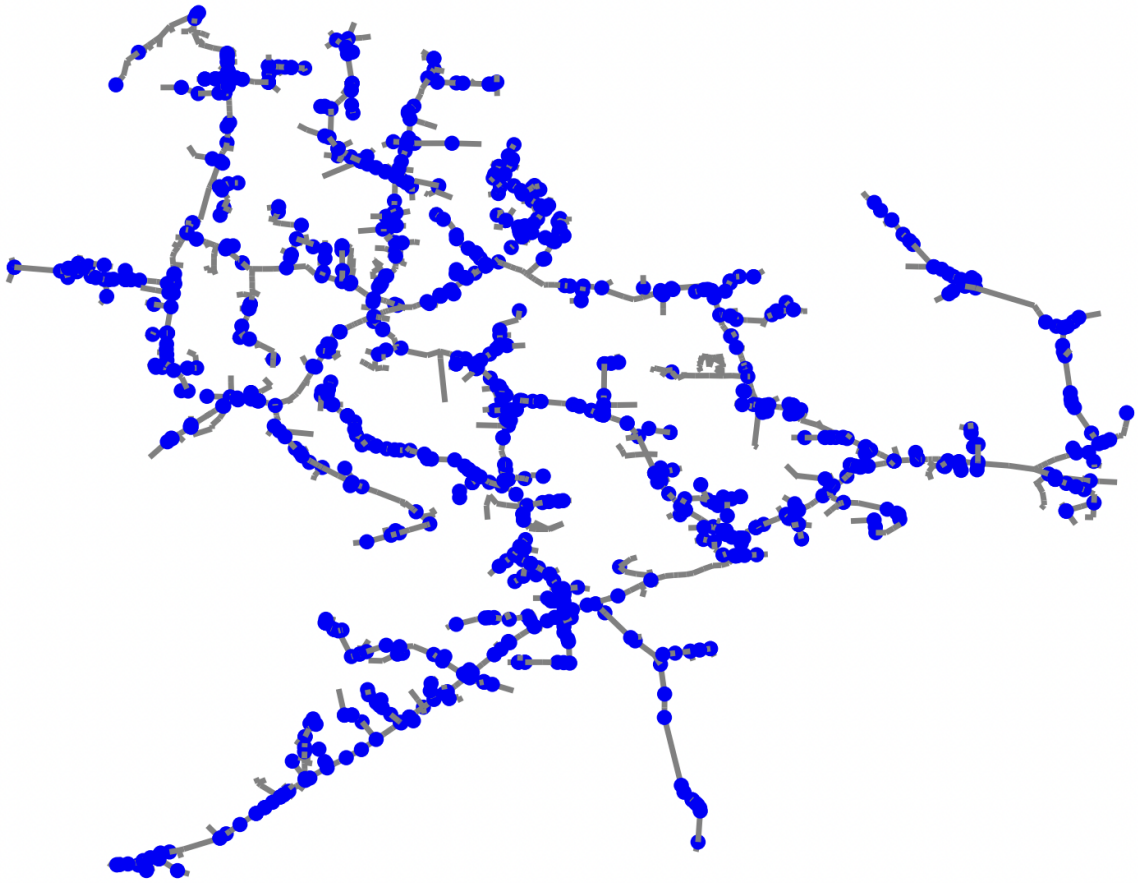

Figure 3.4: A 2522-bus test feeder, modified from the original IEEE 8,500-node feeder, with 3,000 TCL and ESS devices.

3.4.1 Simulation Setup

A 2522-bus (3,817 single-phase nodes) test system as shown in Fig. 3.4, which is extracted from MV-side of the IEEE 8500-node test feeder [SMP+18], is used for numerical case studies. The test system has total of 1,413 single-phase load nodes, where TCLs and ESSs devices are connected and are controlled through Network-

Admissible PEM scheme. Total of 3,000 PEM controlled devices (2,100 TCLs and 900 ESS) are connected to the load nodes. Each load has up to three PEM devices (TCL or ESS), and each device has $P_n^{\text{rate}} = \pm 5\text{kW}$. Different packet lengths are used in the simulation and MTTR is kept same as the packet length. The simulations are run for 1 hour with time step of 2 seconds (i.e., 1,800 time steps).

3.4.2 Performance Metrics

We adopt the following metrics to evaluate the performance of the Network-Admissible PEM.

Composite Performance Score (x_c): This score is used in industry by system operator PJM and measures the overall performance of a grid resource to regulate to the Automatic Generation Control (AGC) reference signal. The performance score is the average of three distinct scores namely, accuracy, delay, and precision scores. For details on scores, please see e [BKOA21].

Voltage Violation Metrics: At the system level, we propose to use the following three voltage violation metrics. Please see [KPAew] for more details on these grid violation metrics.

- **Maximum Duration of Continuous Voltage Violation** (D_m): This metric looks at any node on distribution feeder that exhibits the longest duration of voltage violation, i.e., $\left|V[i_p,k]\right| \geq \overline{V[i_p]} \vee \left|V[i_p,k]\right| \leq \underline{V[i_p]}$.
- **Maximum Cumulative Duration of Voltage Violations** (D_t): Since there exists multiple instances of continuous voltage violation on distribution feeders, D_m alone is not sufficient to capture the temporal distribution of voltage violation. Thus, we propose to use D_t that is the maximum of the cumulative duration of nodal voltage violation.

- **Maximum Area under the Voltage Violation** (A_m): Metrics D_m and D_t defined above only capture the duration of voltage violation; however, these metrics are not able to capture the magnitude of voltage violations. Therefore, we propose to use maximum of cumulative area under the nodal voltage violation function (i.e., area under the voltages above or below the thresholds).

3.4.3 Performance Evaluation

The combined impact of varying packet lengths P_t and grid measurement update rate S_t on the performance metrics are analysed next. To obtain average performance metrics, each case is run 200 times that ensures randomness in the packet requests from TCLs and ESSs. Nodal voltage measurement update rate S_t is varied between 2 seconds, 30 seconds, 2 minutes, and 5 minutes for each of the packet length P_t of 30 seconds, 2 minutes, and 5 minutes.

Fig. 3.5 presents a sample case (one out of 200 runs) in tracking a real AGC signal with varying packet lengths with S_t =2 seconds. The overall situation is better visualized in the Fig. 3.5 inset, where we can see that, with the 30-second packet length the tracking performance is superior, which degrades gradually with 2-minute and 5-minute packet lengths. Fig. 3.6 shows another sample case in tracking AGC by varying measurement update rates (with $P_t = 5$ minutes). The overall situation is better visualized in the Fig. 3.6 inset, where we can see that, the tracking starts deteriorating as S_t is increased gradually from 2 seconds to 5 minutes.

The impact of S_t on system-wide voltage performance is shown in Fig. 3.7 for the sample case of Fig. 3.6. The simulation comprises of 6,870,600 instances of voltage

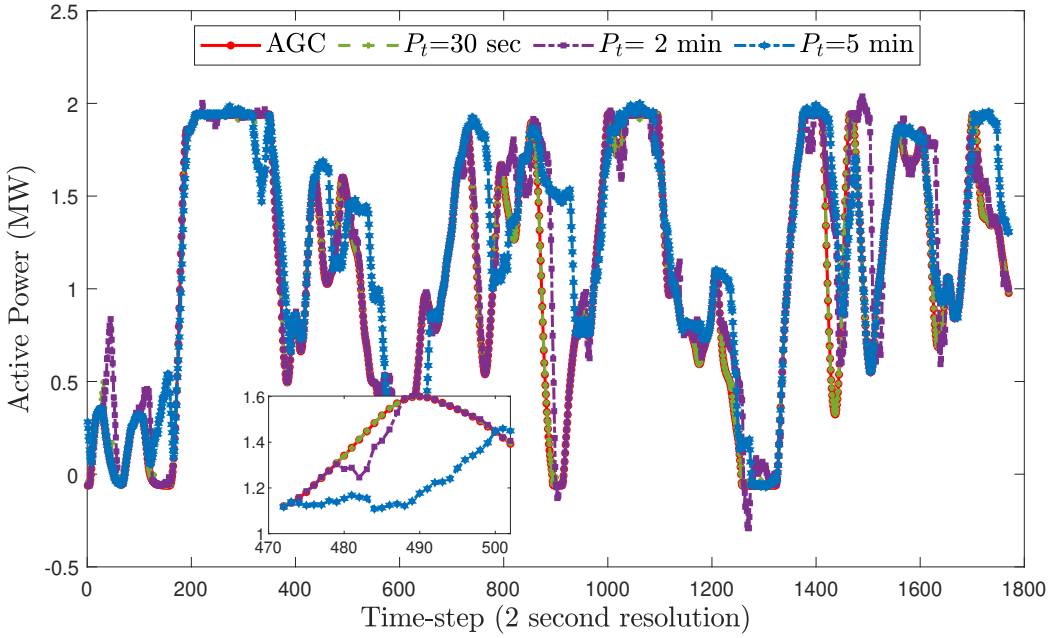

Figure 3.5: Impact of packet length P_t on tracking performance of Network-Admissible PEM with $S_t = 2$ seconds.

that correspond to 1,800 time steps simulation (1 hour) of 3,817 single-phase nodes of the test feeder. For $S_t = 2$ seconds, 130 nodes (5,405 voltage instances) experienced voltage over 1.05 p.u. As S_t is increased to 30 seconds and 2 minutes, the overvoltage instances increased. With $S_t = 5$ minutes, the total nodes with overvoltage increased to 483 (with 62,584 voltage instances).

Fig. 3.8 (a) shows comparison of the maximum duration of continuous voltage violation (D_m), which is averaged over 200 runs for each value of P_t and S_t. For each packet length, as we increase S_t, the duration D_m increases. For example, with $P_t = 30$ seconds, D_m varies from 18 seconds to 240 seconds (out of 3,600 seconds of simulation) by varying S_t. With a coarse P_t (5 minutes), and measurement update rate of $S_t = 5$ minutes, D_m is 372 seconds, which is about 10% of total simulation duration and is significant overvoltage duration. We observed similar trend on

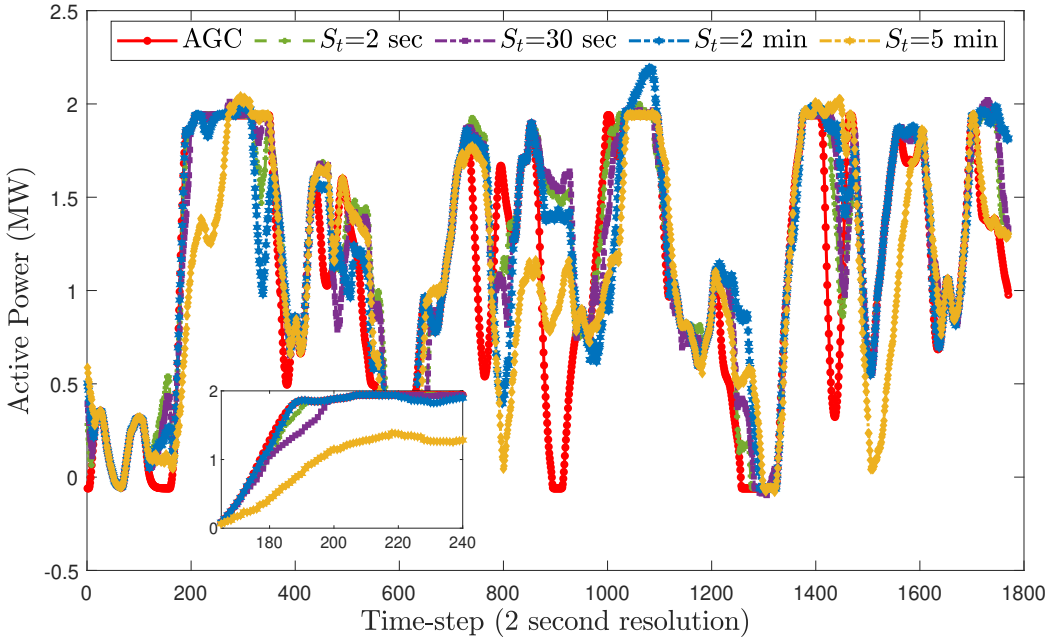

Figure 3.6: Impact of measurement update rate S_t on tracking performance of Network-Admissible PEM with $P_t = 5$ minutes.

maximum cumulative duration of voltage violation metric (D_t) (see Fig. 3.8 (b)) and the area under the voltage violation metric (A_m) (see Fig. 3.8 (c)). We observed from the case studies that both packet length (P_t) and measurement update rate (S_t) impact the voltage performance metrics considerably.

Fig. 3.8 (d) shows the composite score (x_c) in tracking the sample AGC signal. Value of x_c degrades as P_t and S_t are increased. However, the tracking performance is more dependent on the choice of P_t, and less impacted by S_t for a given value of P_t. Though it is preferred to use finer packet length for improved x_c, a packet length of $P_t = 2$ minutes in the Network-Admissible PEM schemes provided acceptable composite score and voltage performance metrics. This observation on composite score corroborates with the findings in previous work with PEM scheme (without grid constraints) [BKOA21]. Though x_c has acceptable value even with $P_t = 5$ minutes,

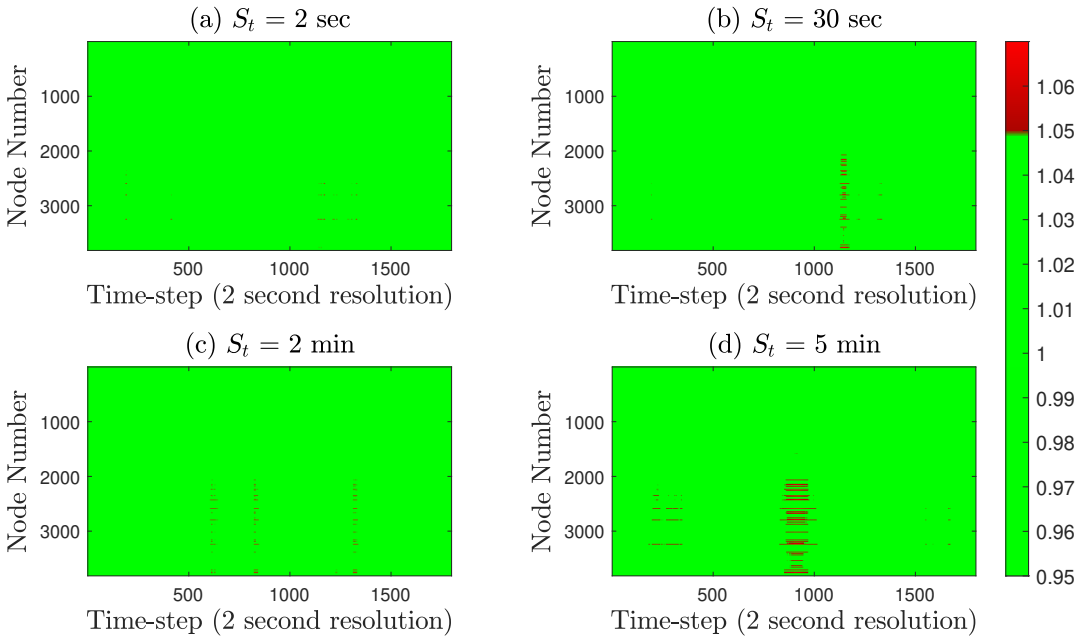

Figure 3.7: System-wide voltage violation on the distribution feeder with varying level of measurement update rate S_t.

this is not advisable from voltage performance point of view. However, if we compliment the coarse packet length with faster grid measurement update rate (e.g., $P_t = 5$ minutes and $S_t = 2$ seconds) we can achieve acceptable voltage performance. Similarly, if PEM uses fine packet length (e.g., $P_t = 30$ seconds), the grid measurements can be updated at slower rate for an acceptable voltage performance.

3.4.4 Impact of Number of Voltage Measurement Buses

The number of voltage measurement buses are changed from 0% (no measurements) to 100% (i.e., all buses with TCLs and ESSs) at a step of 20%. The impact of the number of measurement on the performance metrics is shown in Fig. 3.9 with $P_t = 5$ minutes and $S_t = 2$ seconds for varying number of measurement buses. With no voltage measurement (i.e., equivalent to regular PEM schemes as in [AEHH$^+$18,

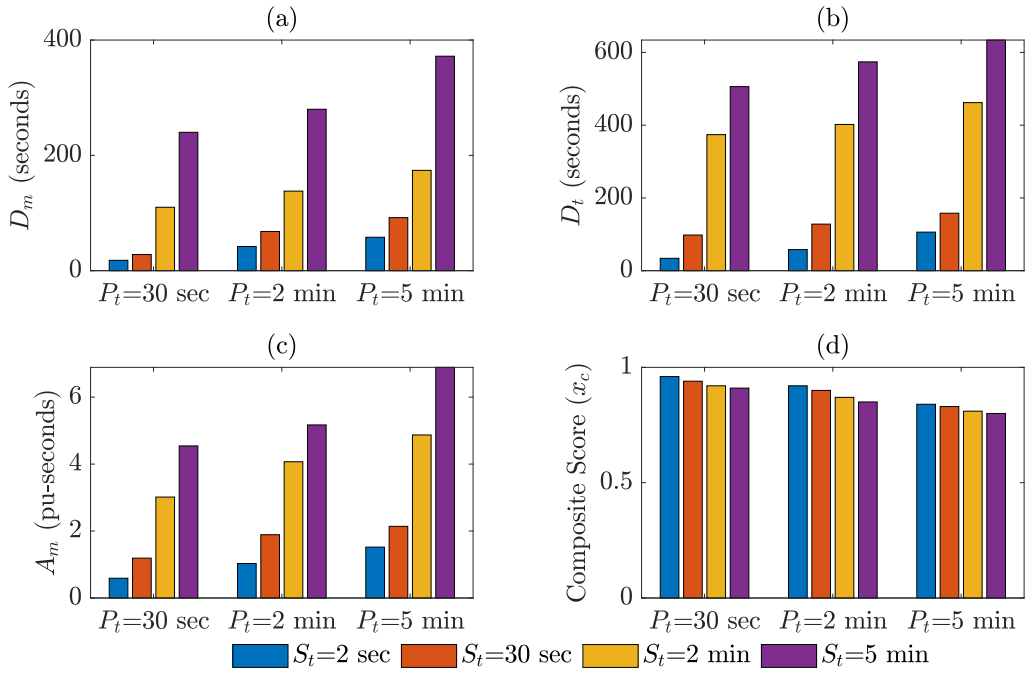

Figure 3.8: Voltage violation metrics (D_m, D_t, and A_m) and composite performance score (x_c) for different values of packet length (P_t) and measurement update rate (S_t).

AFH17]), D_m is 374 seconds (out of 3,600 seconds of simulation), which is significant voltage violation, and reduces to 58 seconds when the grid is fully measured (at TCL and ESS locations). We observed similar trend on D_t and A_m metrics. However, the composite score x_c in tracking AGC almost remained the same with the number of grid measurements.

3.4.5 Impact of Multi-Phase Measurements

As emphasized in section III B, this work evaluates significance of intra-phase voltage measurements on the effective voltage control on single-phase nodes of multi-phase unbalanced feeders. To do so, we have simulated cases with voltage measurements obtained only from the node where PEM devices are connected and compared with

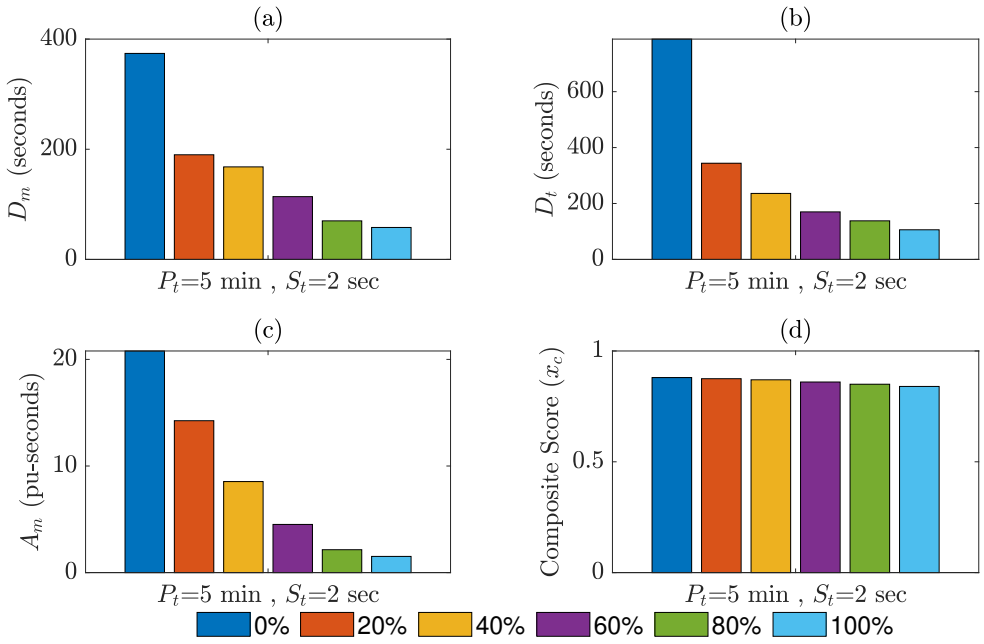

Figure 3.9: Voltage violation metrics (D_m, D_t, and A_m) and composite performance score (x_c) for different number of voltage measurement buses.

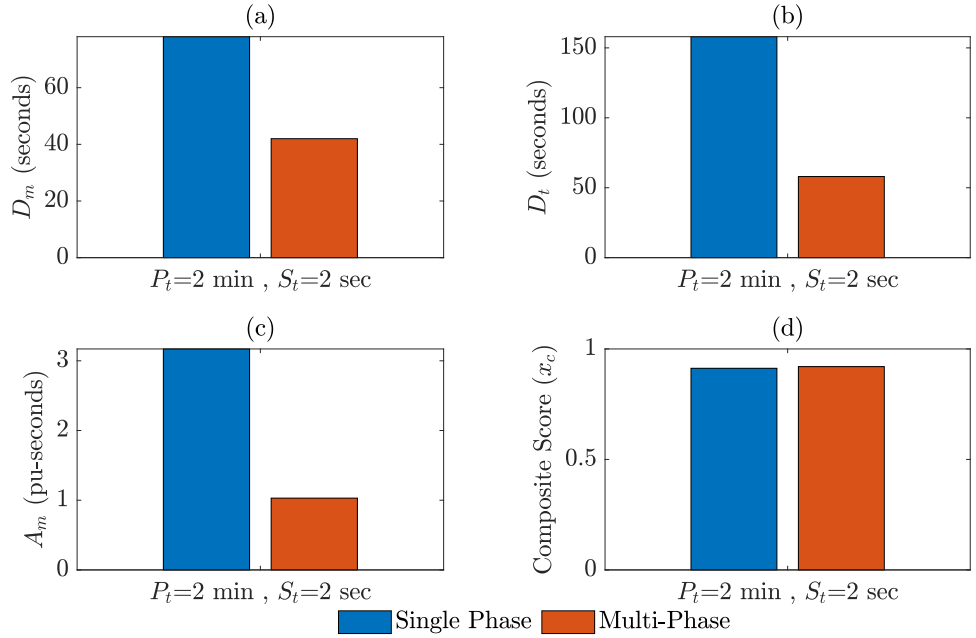

Figure 3.10: a) Voltage violation metrics (D_m, D_t, and A_m) and composite performance score (x_c) for single-phase vs. multi-phase voltage measurements.

multi-phase voltage measurement consideration. The results in Fig. 3.10 shows the comparison of performance metrics with $P_t = 2$ minutes and $S_t = 2$ seconds. Figure shows that all voltage violation metrics are significantly improved when multi-phase measurements are considered. However, like in the other cases, the voltage measurement did not considerably impact the composite score x_c in tracking the reference AGC signal. This case study clearly shows that the single-phase measurement based local voltage control approach is not effective in managing voltages in three-phase unbalanced systems due to the phase coupling effect, whereas intra-phase measurements can ensure better voltage performance in multi-phase distribution feeders.

3.5 Summary

Coordinating demand at scale against variable whole-sale energy market or wide-area control signals requires responsive distributed energy resources (DERs). However, DERs often represent large residential/commercial loads in the distribution system [LM19]. Thus, it is valuable to guarantee that the large-scale coordination of DERs does not violate voltage or current limits or local transformer power ratings. The grid feasibility can also be ensured through the estimation of DER and flexible load hosting capacity as in [WCGW16, JMW16]. In [BBDZ18, SAM19], the grid feasibility is ensured through the design of local droop settings to control active/reactive power of DERs. However, such approaches does not comprehensively take the whole network feasibility and lacks scalability. In this work, we present a network-admissible DER coordination scheme that leverages available live measurements or state estimates. Specifically, for the first time, we analyze how voltage magnitude and apparent power values can be integrated with packetized energy management (PEM), which is a packet-based, randomized control policy for

real-time DER dispatch. This is achieved by considering the device-driven nature of PEM, whereby energy packet requests are made by the devices to the coordinator. The requests are augmented to include grid location and constraint identifiers, which serve together with grid state information to generate a live traffic-like logic table to determine, in real-time, whether packets will be network admissible. This new method is validated on the IEEE test networks for packetized DERs where we show that network-admissible PEM achieves large-scale (global) tracking objectives while abiding by local network constraints. We also study the effect of constraint tightening on reference-tracking performance in the aggregate.

This work provided comprehensive performance evaluation of a demand dispatch algorithm in maintaining grid voltages and tracking reference (e.g., AGC signals). The Network-Admissible demand dispatch represents a generalization of PEM scheme by incorporating new grid constraint management algorithm. This work demonstrated the impact of packet length (in PEM), grid voltage measurement update rate, the number of voltage measurement buses, and multi-phase measurements in managing the grid voltages and in tracking the power reference signal.

Based on the simulation-based analysis carried out in a 2522-bus three-phase unbalanced distribution feeder, we observed that a) the tracking performance is less dependent on grid measurements and is more dependent on the packet length, b) voltage performance depends on both grid measurements and packet length, c) coarse packet length if complemented by fast grid measurement update rate can provide acceptable voltage performance, and d) multi-phase measurements are essential for effective voltage control of multi-phase distribution feeders.

CHAPTER 4

DECOUPLED AND UNIFIED APPROACHES FOR SOLVING TRANSMISSION AND DISTRIBUTION CO-SIMULATIONS

4.1 Introduction

The remainder of the section is structured as following. Section 4.2 provides descriptions on the decoupled and unified approach for solving integrated T&D systems. Section 4.3 discusses the power flow solution methods for transmission and distribution systems. Section 4.4 presents the simulation platform and discusses the adopted evaluation metrics.

Section 4.4 presents and discusses the case studies and simulation results. Section 4.5 presents the main conclusions drawn from this work.

4.2 Decoupled Approach

Consider an $\boldsymbol{N}$-bus transmission system, where the first $\boldsymbol{m}$ buses have lumped loads, and buses $\boldsymbol{m+1}$ through $\boldsymbol{N}$ have distribution feeders connected downstream the buses. In a decoupled approach, power flow model of the transmission system for

the positive sequence can be written as,

$$\boldsymbol{V_j^+ = \sum_{k \in N} Y_{j,k}^+ I_k^+ \quad \forall j \in N} \tag{4.1}$$

$$\boldsymbol{P_j^+ = Real\left(V_j^+ \ I_j^{+*}\right) \ \ \forall j \in 1, 2, .., m} \tag{4.2}$$

$$\boldsymbol{Q_j^+ = Imag\left(V_j^+ \ I_j^{+*}\right) \ \ \forall j \in 1, 2, .., m} \tag{4.3}$$

$$\boldsymbol{\widetilde{P_j^+} = Real\left(V_j^+ \ I_j^{+*}\right) \ \ \forall j \in m+1, .., N} \tag{4.4}$$

$$\boldsymbol{\widetilde{Q_j^+} = Imag\left(V_j^+ \ I_j^{+*}\right) \ \ \forall j \in m+1, .., N} \tag{4.5}$$

$$\boldsymbol{\widetilde{V_j^+} = V_j^+ \ \ \forall j \in m+1, .., N}. \tag{4.6}$$

where $\boldsymbol{V^+}$, $\boldsymbol{I^+}$, $\boldsymbol{P^+}$, $\boldsymbol{Q^+}$, and $\boldsymbol{Y^+}$ represent positive sequence of bus voltage, injection current, active power injection, reactive power injection, and Y-bus matrix, respectively. $\boldsymbol{\widetilde{P_j^+}}$ and $\boldsymbol{\widetilde{Q_j^+}}$ represent equivalent positive sequence lumped load representation of distribution feeders connected at bus $\boldsymbol{j}$. In decoupled approaches, equivalent lumped loads ($\boldsymbol{\widetilde{P^+}}$ and $\boldsymbol{\widetilde{Q^+}}$) are obtained by separately solving the power flow of each distribution systems connected to the transmission network. $\boldsymbol{\widetilde{V^+}}$ represents voltage of transmission buses with distribution feeders downstream the buses.

Consider a $\boldsymbol{R}$-node distribution system connected to an arbitrary $\boldsymbol{j}$-bus of the transmission network. Without loss of generality, we assumed the first three nodes as three-phase sub-station when analyzing the distribution system. Distribution power flow analysis can be formulated similar to the transmission system, except the distribution systems are modeled in phase frame of reference.

$$\boldsymbol{V_i^{\phi}} = \sum_{\boldsymbol{r \in R}} \boldsymbol{Y_{i,r}^{\phi}\, I_r^{\phi}} \quad \forall\, \boldsymbol{i \in R} \tag{4.7}$$

$$\boldsymbol{P_i^{\phi}} = \boldsymbol{Real}\left(\boldsymbol{V_i^{\phi}\ I_i^{\phi *}}\right) \ \ \forall\, \boldsymbol{i \in R} \tag{4.8}$$

$$\boldsymbol{Q_i^{\phi}} = \boldsymbol{Imag}\left(\boldsymbol{V_i^{\phi}\ I_i^{\phi *}}\right) \ \ \forall\, \boldsymbol{i \in R} \tag{4.9}$$

$$\widetilde{\boldsymbol{P_j^{+}}} = -\,\boldsymbol{\mathcal{S}}\left(\boldsymbol{P_1^{\phi}, P_2^{\phi}, P_3^{\phi}}\right) \tag{4.10}$$

$$\widetilde{\boldsymbol{Q_j^{+}}} = -\,\boldsymbol{\mathcal{S}}\left(\boldsymbol{Q_1^{\phi}, Q_2^{\phi}, Q_3^{\phi}}\right) \tag{4.11}$$

$$\left[\boldsymbol{V_1^{\phi}, V_2^{\phi}, V_3^{\phi}}\right] = \boldsymbol{\mathcal{G}}\left(\widetilde{\boldsymbol{V_j^{+}}}\right). \tag{4.12}$$

where $\boldsymbol{V^{\phi}}$, $\boldsymbol{I^{\phi}}$, $\boldsymbol{P^{\phi}}$, and $\boldsymbol{Q^{\phi}}$ represent node voltage, injection current, active power injection, and reactive power injection, respectively, in phase frame of reference. $\boldsymbol{Y^{\phi}}$ represents Y-bus matrix of a three-phase system in phase frame of reference. Functions $\boldsymbol{\mathcal{S}}$ ( ) and $\boldsymbol{\mathcal{G}}$ ( ) convert powers on three phases to positive sequence power and positive sequence voltage to three-phase voltages, respectively. These conversions assume that the transmission system is balanced; hence, the three-phase voltages at the sub-station nodes ($\boldsymbol{V_1^{\phi}}$, $\boldsymbol{V_2^{\phi}}$, $\boldsymbol{V_3^{\phi}}$) of the distribution system are balanced.

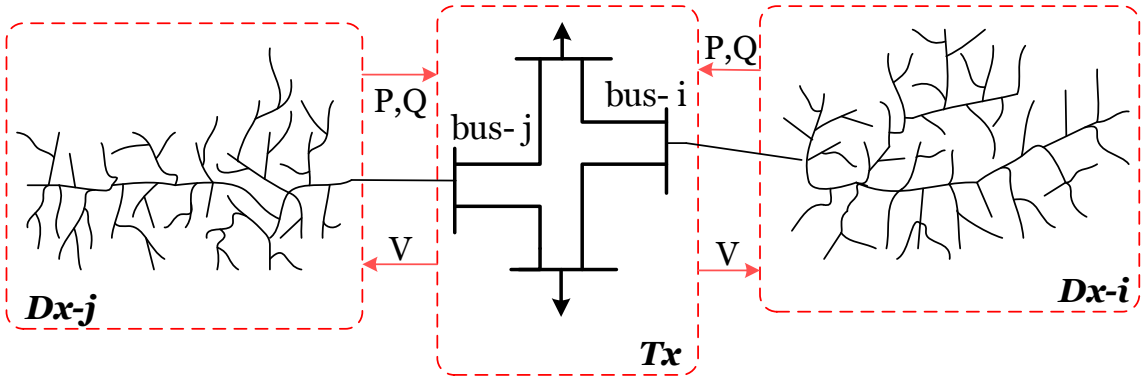

Figure 4.1: A T&D system showing boundaries and information exchange for solving transmission (Tx) and distribution (Dx) co-simulation using a decoupled approach.

The solution procedure of mathematical models (1)-(12) of the decoupled approach can be explained using Fig. 4.1. In the Fig. 4.1, an integrated T&D system is shown where distribution feeders are connected at nodes $\boldsymbol{i}$ and $\boldsymbol{j}$. In the decoupled approach, the transmission and distribution systems are solved iteratively and based on some information exchange. First, assuming a nominal sub-station voltages, power flow model (7)-(11) are solved for each distribution systems in phase frame of reference. This provides total active and reactive power consumed by each distribution feeders (including losses) and are converted to positive sequence powers. Now with this information from all distribution circuits, the distribution systems are represented as lumped loads on respective transmission buses and transmission system power flow model (1)-(6) are solved. Solution of this provides positive sequence bus voltages, which are then converted to voltages in phase frame of reference using (12). The bus voltage obtained from transmission power flow in phase frame are used to update the distribution system three-phase substation voltage using (12) and distribution level power flow models (7)-(11) are solved again for each distribution systems. These transmission and distribution power flow models are solved iterative using P,Q,V updates until the convergence criterion is met.

4.3 Unified Approach

4.3.1 Power Flow Model

In this section, an integrated transmission and distribution system model is developed and a unified load flow which runs for combined system is discussed. Our Unified approach considers transmission as a balanced system and distribution as unbalanced system. Therefore, we used positive sequence for transmission system

and all three-sequence network for distribution system analysis. The distribution system represented using three phase parameters is converted to sequence frame and combined with transmission system parameters to develop an integrated T&D system.

Consider an $\boldsymbol{N}$-bus transmission system connected to $\boldsymbol{M}$-bus distribution system. In unified approach, power flow model of the combined system for the positive sequence can be written as,

$$\boldsymbol{V_j^+} = \sum_{\boldsymbol{k \in N+M}} \boldsymbol{Y_{j,k}^+ \, I_k^+} \quad \forall \, \boldsymbol{j \in N+M} \tag{4.13}$$

$$\boldsymbol{P_j^+} = \boldsymbol{Real}\left(\boldsymbol{V_j^+ \; I_j^{+*}}\right) \quad \forall \, \boldsymbol{j \in 1, 2, .., N+M} \tag{4.14}$$

$$\boldsymbol{Q_j^+} = \boldsymbol{Imag}\left(\boldsymbol{V_j^+ \; I_j^{+*}}\right) \quad \forall \, \boldsymbol{j \in 1, 2, .., N+M.} \tag{4.15}$$

where $\boldsymbol{V^+}$, $\boldsymbol{I^+}$, $\boldsymbol{P^+}$, $\boldsymbol{Q^+}$, and $\boldsymbol{Y^+}$ represent positive sequence of bus voltage, injection current, active power injection, reactive power injection, and positive sequence Y-bus matrix. Transmission system parameters are readily available in sequence frame of reference, while the three-phase distribution impedance parameters need to be converted to sequence impedances. The formulation can be readily extended to include the negative and zero sequence component circuits for distribution grid. The distribution three-phase parameters are converted to three-sequence details using a stacked Y-bus methodology. Then, the sequence Y-bus of distribution system is combined with the sequence Y-bus of transmission system to obtain integrated T&D Y-bus. The load data of integrated system is per unitized to a common base which is used with integrated Y-bus to begin load flow analysis. Newton Raphson method is used to solve load flow. Since the distribution system considered in this work is a balanced system, the Newton Raphson method would converge for the combined system. A flow chart of the unified simulation of integrated T&D system is presented in Fig. 4.2.

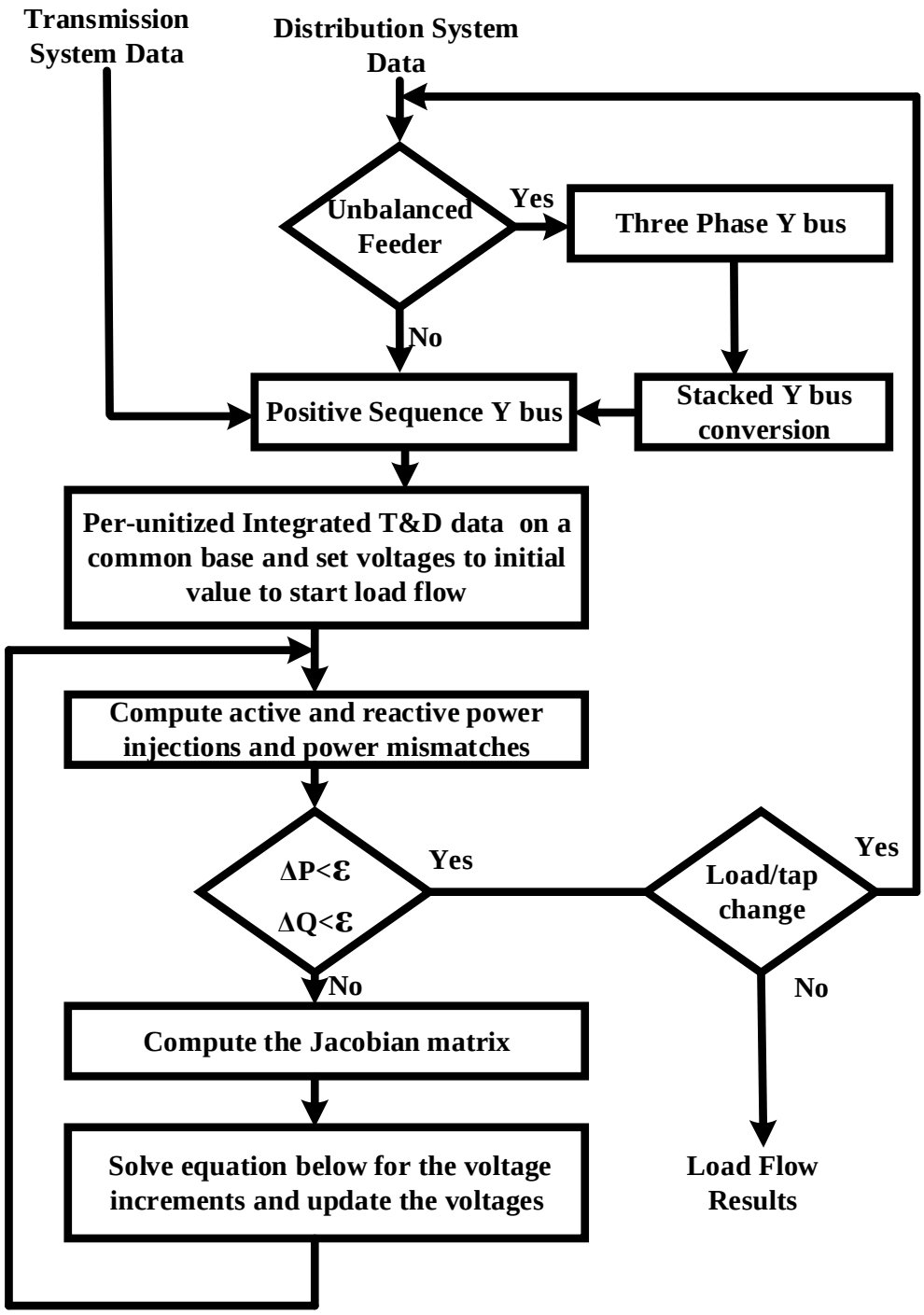

Figure 4.2: Flowchart of Unified T&D Simulation.

4.3.2 Y-bus in Sequence Frame

The stacked Y-bus methodology builds from the admittance matrices of individual elements. We briefly discuss the formation of admittance matrix of individual series components next. Note that even though the formulation is shown only for a generic conductors/cables and transformer models, we consider a comprehensive set of series elements (e.g., 1-phase feeders, 2-phase feeder, 3-phase feeders, 1-phase and 3-phase load tap changers, delta–wye/wye–delta/ wye–wye/ delta–delta transformers, 1-phase transformers, etc.).

For typical multi-phase cables and conductors connected between node n and node m, component of 3-phase Y-bus can be obtained as,

$$\mathbf{Y}_{nn} = \mathbf{Y}_{mm} = \frac{1}{2}\mathbf{B}_{nm} + \mathbf{Z}_{nm}^{-1} \tag{4.16}$$

$$\mathbf{Y}_{nm} = \mathbf{Y}_{mn} = \mathbf{Z}_{nm}^{-1}. \tag{4.17}$$

Similarly, a three-phase transformer can be represented by a series block representing the per unit leakage admittance, and a shunt block modeling transformer core losses. The nodal admittances of different connections types of transformer are shown in Table 4.1.

Table 4.1: Y-bus for Various Transformer Connections.

Node n	Node m	Ynn	Ynm	Ymn	Ymm
Wye-G	Wye-G	Y1	Y1	Y1	Y1
Wye	Wye	Y2	Y2	Y2	Y2
Wye	Delta	Y2	-Y3	$-Y3^T$	Y2
Delta	Delta	Y2	Y2	Y2	Y2

$$\mathbf{Y}_1 = \begin{bmatrix} y_t & 0 & 0 \\ 0 & y_t & 0 \\ 0 & 0 & y_t \end{bmatrix}, \mathbf{Y}_2 = \frac{1}{3}\begin{bmatrix} 2y_t & -y_t & -y_t \\ -y_t & 2y_t & -y_t \\ -y_t & -y_t & 2y_t \end{bmatrix} \tag{4.18}$$

$$\mathbf{Y}_3 = \frac{1}{\sqrt{3}}\begin{bmatrix} -y_t & y_t & 0 \\ 0 & -y_t & y_t \\ y_t & 0 & -y_t \end{bmatrix}, \mathbf{Y}_4 = \frac{1}{3}\begin{bmatrix} y_t & -y_t & 0 \\ -y_t & 2y_t & -y_t \\ 0 & -y_t & y_t \end{bmatrix} \tag{4.19}$$

$$\mathbf{Y}_5 = \begin{bmatrix} y_t & 0 \\ 0 & y_t \end{bmatrix}, \mathbf{Y}_6 = \frac{1}{\sqrt{3}}\begin{bmatrix} -y_t & y_t & 0 \\ 0 & -y_t & y_t \end{bmatrix}. \tag{4.20}$$

where y_t is the per unit leakage admittance.

After the admittance matrices for individual series components are computed, stacked Y-bus method can be used as following,

- Using 3-phase primitive Y-bus for individual component, built 3-phase Y-bus of distribution system .
- Take each 3x3 matrix from the 3-phase Y-bus.
- Find inverse to obtain Z.
- Convert Z to sequence components.
- Inverse the sequence impedance components to obtain sequence admittance component.
- Append this distribution system sequence Y-bus to positive sequence Y-bus of transmission system to obtain Y-bus of integrated T&D system.

Voltage Regulators

The voltage regulators are generally in series with a transmission line. Knowing the value of regulator taps, Ybus components for voltage regulator and line as a single

block between nodes m and n can be obtained as in [BG18a] using equation below.

$$\mathbf{Y}_{nn} = \mathbf{A}_{\mathrm{i}}\mathbf{F}_{\mathrm{R}}^{-1}\mathbf{Y}_{nn}\mathbf{A}_{\mathrm{i}}^{T} \tag{4.21}$$

$$\mathbf{Y}_{nm} = \mathbf{A}_{\mathrm{i}}\mathbf{F}_{\mathrm{R}}^{-1}\mathbf{Y}_{nm} \tag{4.22}$$

$$\mathbf{Y}_{mn} = \mathbf{Y}_{mn}\mathbf{F}_{\mathrm{R}}^{-T}\mathbf{A}_{\mathrm{i}}^{T} \tag{4.23}$$

$$\mathbf{Y}_{mn} = \mathbf{Y}_{mm} - \mathbf{Y}_{mn}\mathbf{A}_{\mathrm{i}}^{T}\mathbf{Z}_{\mathrm{R}}\mathbf{A}_{\mathrm{i}}\mathbf{F}_{\mathrm{R}}^{-1}\mathbf{Y}_{nm} \tag{4.24}$$

where Ai is current gain matrix and ZR is impedance matrix and FR is given by

$$\mathbf{F}_{\mathrm{R}} = \mathbf{I} + \mathbf{Y}_{nm}\mathbf{A}_{\mathrm{i}}^{T}\mathbf{Z}_{\mathrm{R}}\mathbf{A}_{\mathrm{i}} \tag{4.25}$$

$$\mathbf{A}_{\mathrm{i}} = \begin{bmatrix} \frac{1}{a_{R_a}} & 0 & 0 \\ 0 & \frac{1}{a_{R_b}} & 0 \\ 0 & 0 & \frac{1}{a_{R_c}} \end{bmatrix}. \tag{4.26}$$

$$\mathbf{Z}_{\mathrm{R}} = \begin{bmatrix} z_{R_a} & 0 & 0 \\ 0 & z_{R_b} & 0 \\ 0 & 0 & z_{R_c} \end{bmatrix}. \tag{4.27}$$

$$a_R = 1 \mp 0.00625\texttt{tap}. \tag{4.28}$$

4.4 Case Studies

4.4.1 Validation of Power Flow Models

A current injection method similar to [dMP99] is used to solve the power flow models, where the current injection equations are written in rectangular coordinates. In the current injection method, the Jacobian matrix has the same structure as the nodal

admittance matrix except for PV buses. Off-diagonal blocks of the Jacobian matrix are equal to those of the nodal admittance matrix. The diagonal blocks are updated according to type of load model considered for that bus. For each PV bus, a new dependent variable is introduced with an additional equation imposing zero bus voltage deviation.

An integrated T&D system is formed by combining a 14-bus transmission system and a 33-node balanced distribution system connected to as shown in Fig. 4.3. The 14-bus transmission system consists of 5 generators and 11 loads with net load of 260MW (75MVAr). The 33-node distribution system has net connected load of 3.7MW (2.3MVAr). First, the transmission system model and distribution system model are separately verified for the distributed approach. The transmission system

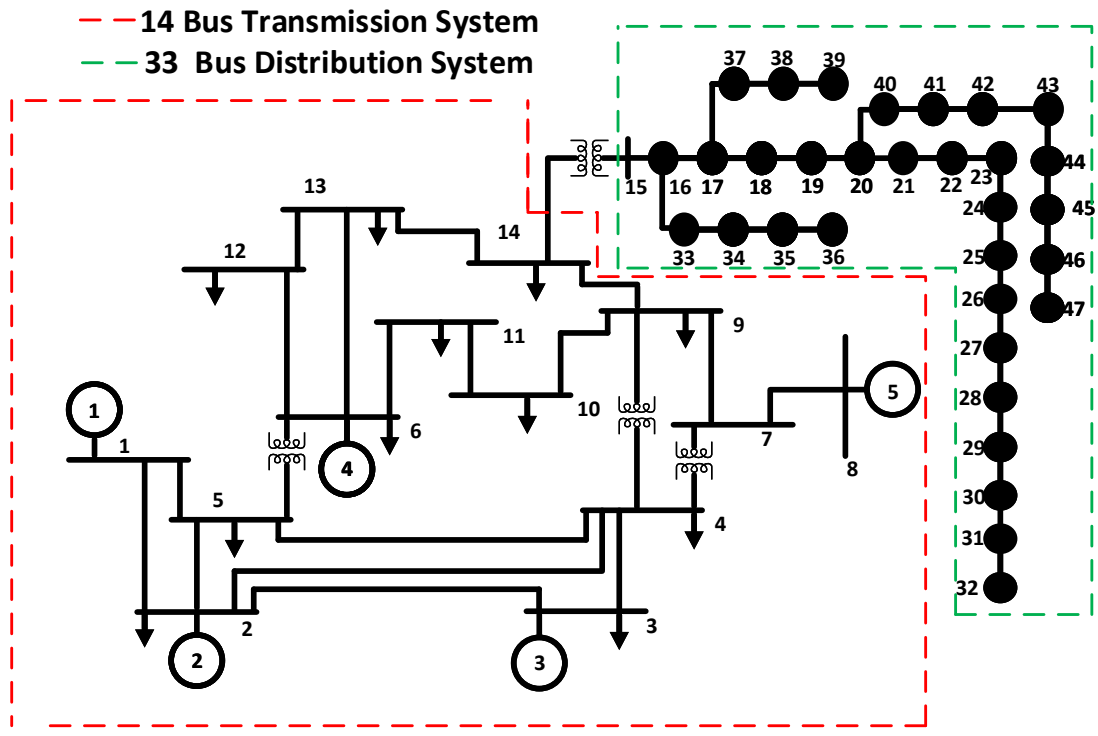

Figure 4.3: One line diagram of 47-bus T&D system.

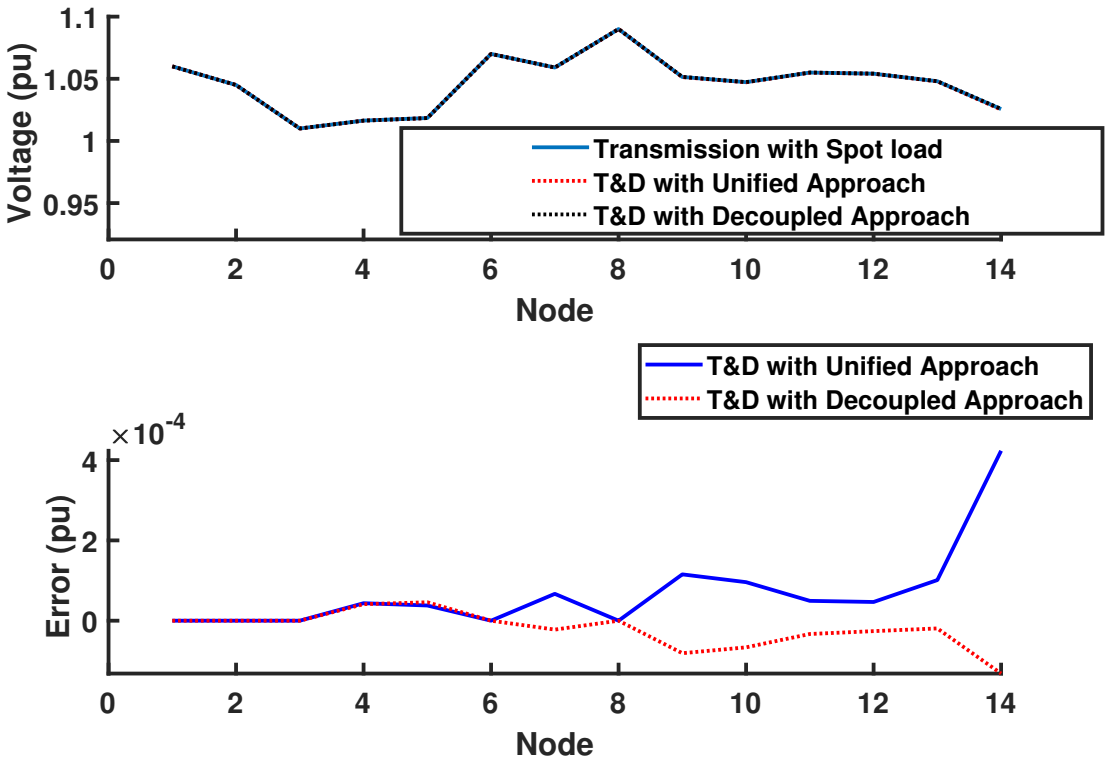

Figure 4.4: Voltage solution and error on transmission circuits.

model is also solved with spot load approach, where all the loads on distribution feeders are lumped at a corresponding transmission bus. Then, the combined T&D model is solved using distributed and unified approach, and the results are shown in Fig.4.7. The error plot shows that the decoupled approach results is the same solution as the unified approach.

4.4.2 47-bus System

The augmented 47-bus system (see Fig. 4.3) is further used to compare the performance of voltage and power angle solution on the transmission as well as distribution

part of the circuit. The load flow voltage and angle obtained from the unified approach and decoupled approach are shown in Fig. 4.5 and Fig. 4.6. The plots clearly show that the voltage and angle solutions from both approaches are very close with error less than 6×10^{-6} on voltages and 2.5×10^{-3} on angles.

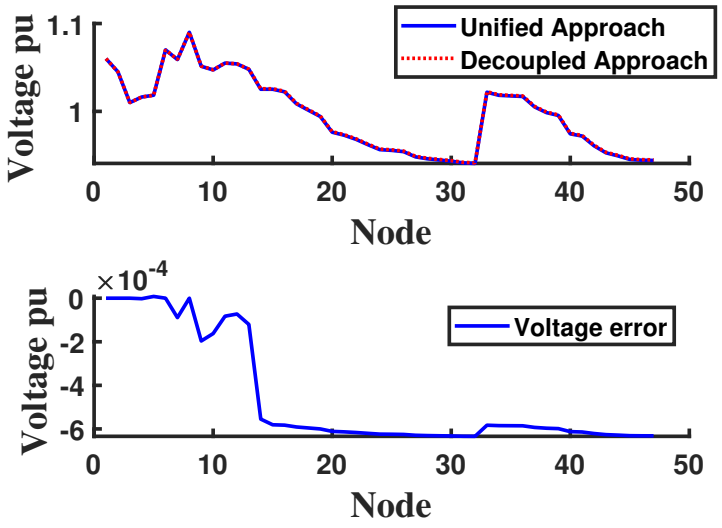

Figure 4.5: Voltage solution (and error) of 47-bus T&D system obtained from decoupled and unified approaches.

4.4.3 113-bus System

Two augmented 113-bus systems are created by using three sections of 33-node distribution feeder (see Fig. 4.7). The load flow voltage and angle obtained from the unified approach and decoupled approach for the first case of the circuit configuration (Case a) are shown in Fig. 4.8 and Fig. 4.9. The plots clearly show that the voltage and angle solutions from both approaches are very close with error less than 3×10^{-5} on voltages and 2.5×10^{-3} on angles. For the second case of the circuit configuration (Case b), the voltage and angle solution obtained are shown in Fig. 4.10 and Fig. 4.11. The plots clearly show that the voltage and angle solutions from both

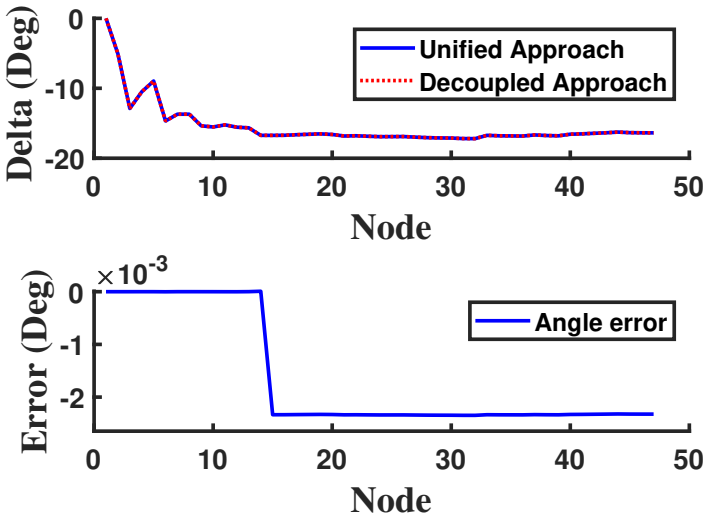

Figure 4.6: Angle solution (and error) of 47-bus T&D system obtained from decoupled and unified approaches.

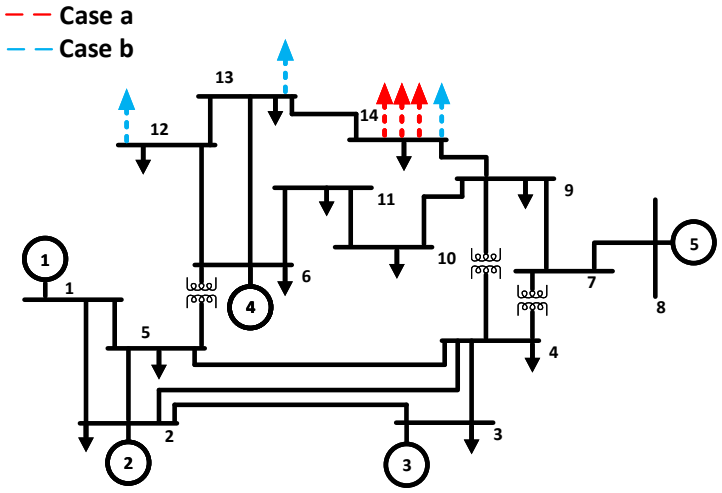

Figure 4.7: Two configuration of 113-bus T&D system.

approaches are very close with error less than 3×10^{-5} on voltages and 2.5×10^{-3} on angles. The case studies demonstrate that the distributed and unified approaches for solving T&D model yield the same solutions.

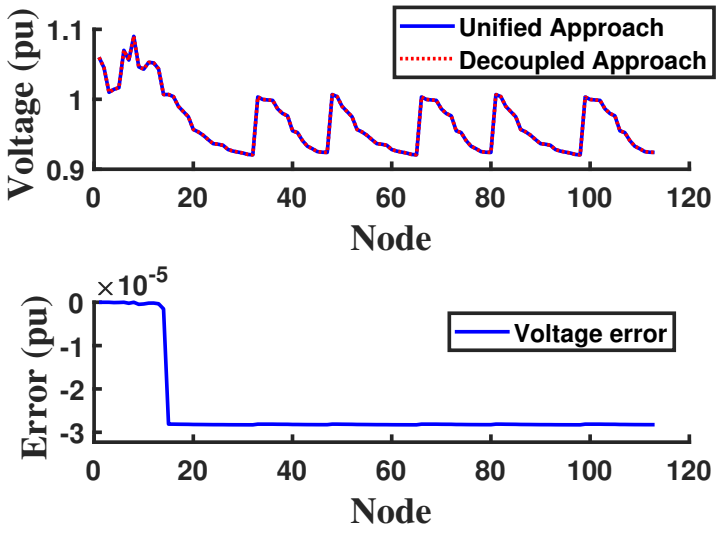

Figure 4.8: Voltage solution (and error) of 113-bus T&D system (Case a) obtained from decoupled and unified approaches.

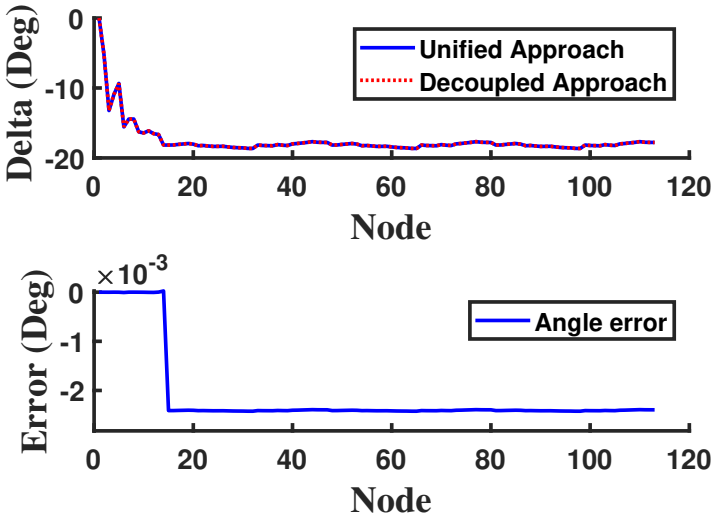

Figure 4.9: Angle solution (and error) of 113-bus T&D system (Case a) obtained from decoupled and unified approaches.

4.5 Summary

Traditionally, the transmission systems and distribution systems are solved independently and using the off-the-shelf simulators. In conventional simulation tools,

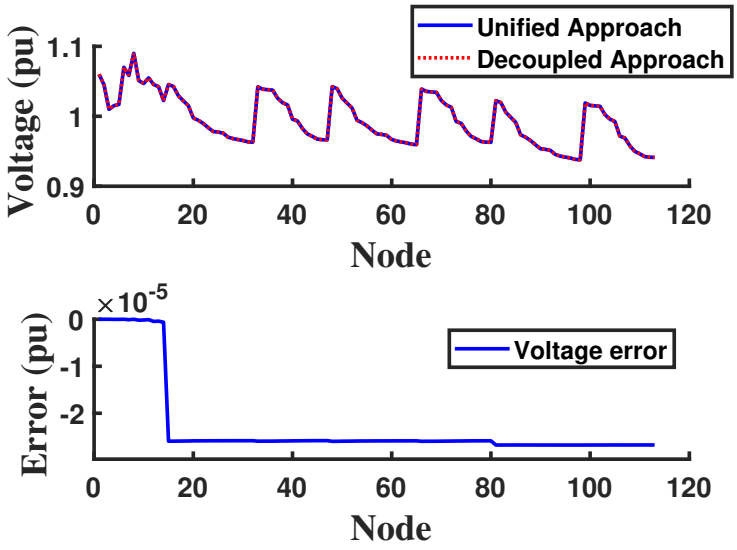

Figure 4.10: Voltage solution (and error) of 113-bus T&D system (Case b) obtained from decoupled and unified approaches.

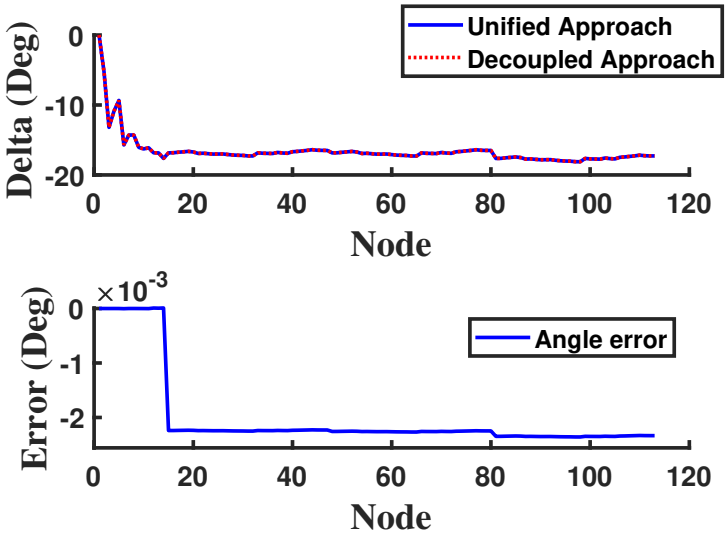

Figure 4.11: Angle solution (and error) of 113-bus T&D system (Case b) obtained from decoupled and unified approaches.

transmission and distribution circuits are treated as separate systems and are analyzed independently. In such tools, distribution systems are represented by lumped loads while solving the transmission system. On the other hand, the transmission

system is represented using a constant voltage source while solving distribution circuits [JB18, HV17, HFD$^+$17, BA17]. Our case studies on small scale 47-bus and 113-bus T&D systems show that the decoupled approach are fairly accurate compared to the unified approaches for solving T&D co-simulation. However, our observation is based on synthetic small-scale system; thus, extensive simulations on large scale systems with three-phase unbalanced distribution grids must be considered before making any generic conclusion regarding the accuracy of decoupled approaches. Therefore, we tackle this issue in the next chapter.

CHAPTER 5

GPU-BASED EFFICIENT LARGE-SCALE SIMULATION OF INTEGRATED TRANSMISSION AND DISTRIBUTION SYSTEMS

5.1 Introduction

The remainder of the section is structured as following. Section 5.2 provides descriptions on the CPU-GPU-based power flow method for solving integrated T&D systems. Section 5.3 discusses simulation tool, GPU architecture, and CPU-GPU hybrid implementation discusses the adopted evaluation metrics. Section 5.4 presents and discusses the case studies and simulation results. Section 5.5 presents the main conclusions drawn from this work.

5.2 Power Flow Solution Methods

In this Section, we briefly explain the two power flow solution algorithms used for the transmission and distribution systems. There are derivative-free methods to solve distribution system power flow, which are demonstrated to be efficient for large-scale systems and are suitable for GPU implementation. However, the main computational bottleneck would be from the power flow of transmission side, which we overcome using an Inexact Newton Method.

5.2.1 Inexact Newton Method

Being a derivative based method that requires minimal effort on the initial guess and excellent convergence for transmission level power flow, NR is typically used over others [BGMEA76, DMJK08]. However, NR is slow for large systems. In regular NR method, the power flow solution is obtained by solving iteratively the following set

of equations with mismatch vector $[\Delta x]$, Jacobian matrix $[J]$, and unknown vector $[\Delta y]$.

$$\underbrace{\begin{bmatrix} \Delta P \\ \Delta Q \end{bmatrix}_k}_{[\Delta x]} = \underbrace{\begin{bmatrix} J_1 & J_2 \\ J_3 & J_4 \end{bmatrix}_k}_{[J]} \underbrace{\begin{bmatrix} \Delta \delta \\ \Delta V \end{bmatrix}_k}_{[\Delta y]} \tag{5.1}$$

where $J_1 = \frac{\partial P}{\partial \delta}$, $J_2 = \frac{\partial P}{\partial V}$, $J_3 = \frac{\partial Q}{\partial \delta}$, $J_4 = \frac{\partial Q}{\partial V}$. P, Q, V, δ are the active, reactive power, voltage magnitude and angle respectively. The k-th iteration of NR update equations can be written as,

$$[x_{k+1}] = [x_k] + [\Delta x_k], \tag{5.2}$$

$$[\Delta x_k] = [J_k]^{-1} [\Delta y_k]. \tag{5.3}$$

Computational burden of NR depends on the size of Jacobian sub-matrices $[J1]$, $[J2]$, $[J3]$, $[J4]$ in (5.1) and factorization of the full Jacobian matrix at every iteration. For large system (thousands of buses) the burden is huge as the weight of the matrix increases in a cubic rate of matrix size N. Though the factorization operation of the matrix can be reduced to $N^{1.5}$ from N^3 using sparse matrices techniques, still around 85% time and computational resources are consumed by these factorization and remains the most critical issue in solving large-scale power systems with NR method [Mil10]. Therefore, in this work, Inexact Newton method is used to reduce the computational burden and to achieve faster solve time. In the Inexact Newton method, the Jacobian matrix is pre-calculated and kept constant throughout the iterative process, which is proven to be fairly accurate, and computationally less burdensome. This also makes the GPU implementation much simpler as avoid large matrix inversion every iteration. The update equation can be written as,

$$[x_{k+1}] = [x_k] + [\Delta x_k], \tag{5.4}$$

$$[\Delta x_k] = [\bar{J}]^{-1} [\Delta y_k], \tag{5.5}$$

where $[\bar{J}]$ is the Jacobian matrix which is kept constant through the NR update process, and is equal to the Jacobian matrix evaluate at the initial starting solution of NR.

5.2.2 Z-Bus Method

On the distribution system side, derivative free methods are available. We adopt Implicit Z-bus method, which is derivative free, and hence, simple to implement and has shown efficient computational performance [CCH$^+$91]. Implicit Z-bus methods involve the solution of a linear set of equations for constant current injections and an iterative method for representing non-linear constant power load models [CCH$^+$91].

The basic of Implicit Z-bus method follows ohm's law in a circuit and in the three-phase frame can be represented as,

$$\underbrace{\begin{bmatrix} i_n \\ i_s \end{bmatrix}}_{[i]} = \underbrace{\begin{bmatrix} Y_{NN} & Y_{NS} \\ Y_{SN} & Y_{SS} \end{bmatrix}}_{[Y]} \underbrace{\begin{bmatrix} v_n \\ v_s \end{bmatrix}}_{[v]} \quad (5.6)$$

where $[Y]$ is the network admittance that consists of four sub-matrices of Y_{NN}, Y_{SN}, Y_{NS} and Y_{SS}. Subscript S represents slack buses and N represents non-slack buses. $[i]$ is the nodal current injection vector, and $[v]$ is the nodal voltage vector. The voltage update equation of Z-bus is given as,

$$v_n = {Y_{NN}}^{-1} i_n - {Y_{NN}}^{-1} Y_{NS}\ v_s. \quad (5.7)$$

5.3 Simulation Tool and Evaluation Metrics

The simulation models are run on CPU and GPU using Microsoft Visual Studio Integrated development environment (IDE) (version 2017 community). The CPU

operating environment comprises 64 bit 8th Generation Intel® Core™ i7 6 core and 12 threads (6C12T) Processors running at 2.20 GHz, and Bus Speed of 8 GT/s. The maximum memory size is 64 GB in a maximum of 2 channels with a maximum memory bandwidth of 41.8 GB/s. The GPU is an NVIDIA GeForce GTX 1050 Ti (4 GB, DDR5) with 768 CUDA cores with a Processor clock of 1.392 GHz, a Graphics Clock of 1.290 GHz, and a Memory Bandwidth of 112 GB/s connected through a 128-bit wide memory PCIe.

5.3.1 GPU Architecture and CUDA

A typical GPU has a design specific number (N) of Streaming Multiprocessors cores (SMs). SMs are the highest architectural component within the structure that comprises streaming processors (SP), registers, and on-chip low latency shared memory (used for local variables) as shown in Fig. 5.1. Each SP comprises of integer and single-precision floating point units. Each SM has 1 double-precision floating-point unit and 2 single-precision transcendental function (special function, SF) units shared the SPs in the SM. All the on-chip SPs share the larger off-chip memory called to as device or global memory that is accessible by all MPs [NVI10].

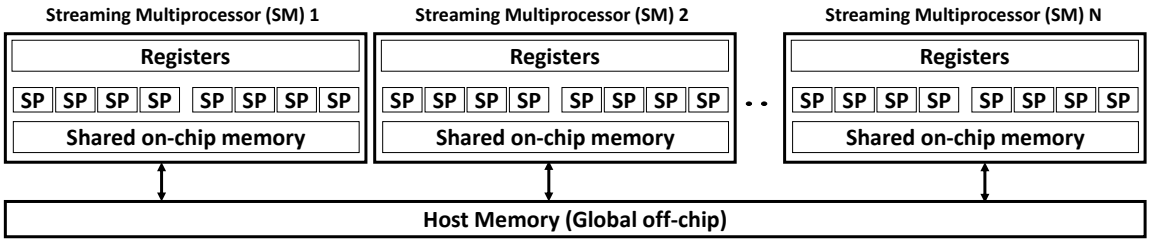

Figure 5.1: A general architecture of a GPU.

In this work, we are using a NVIDIA GPU and the algorithm is based on Compute Unified Device Architecture (CUDA) based application program inter-

faces (API) which is a simpler device management when using NVIDIA GPUs [FVS11, SCL+12, KH10]. CUDA is a parallel computing platform and programming model that follows data-parallel model of computation. In the heterogeneous CPU-GPU hybrid CUDA computing environment, the CPU works as a host, processing the sequential (non-iterative) tasks due to its hierarchy in control logic and memory power, and GPU provides the acceleration through accessing the global memory and parallelizing the assigned tasks into multiple SMs through simple logical functions called the kernel which can work in iterative manner [GJY+12]. The typical execution model of a CUDA program is shown in Fig. 5.2 where CPU, the host, initiates the simulation process and transfers the calculation instruction and

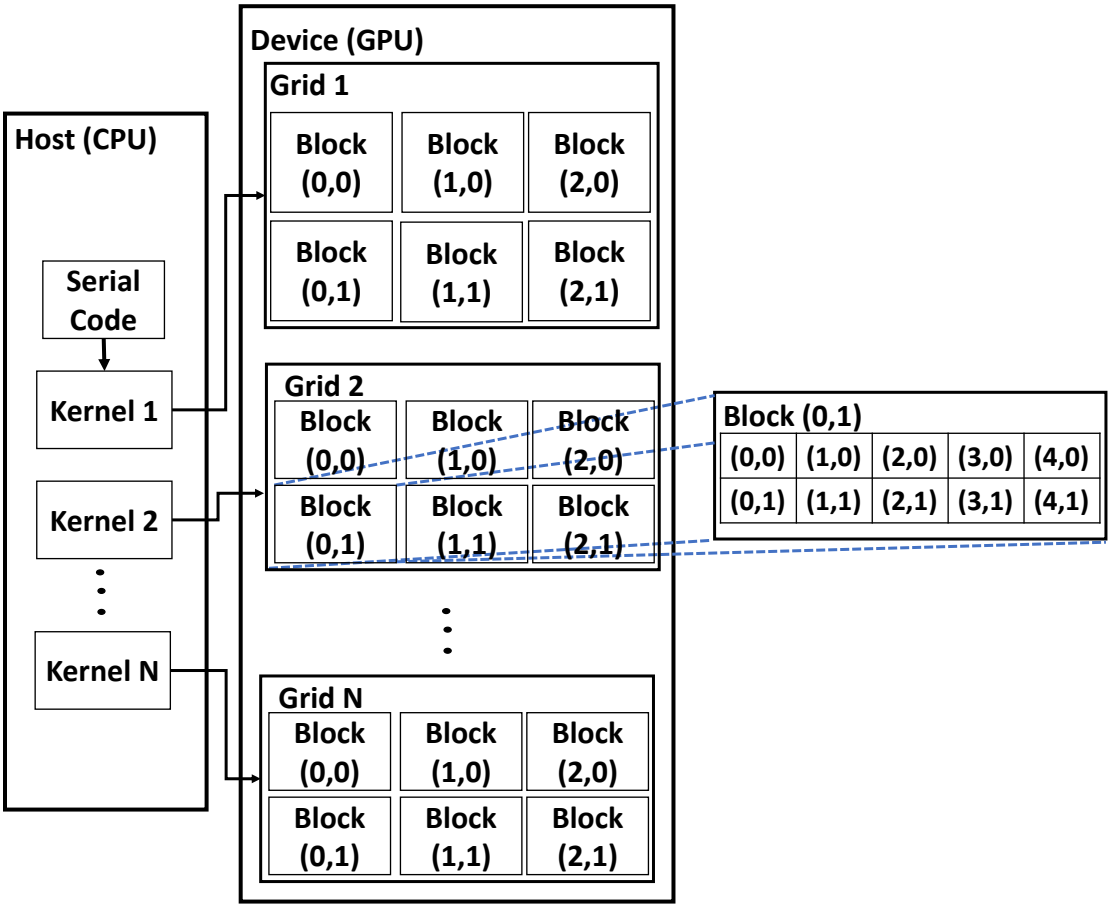

Figure 5.2: Schematic illustration of CUDA programming elements.

parameters to the GPU by initiating kernel calls which in turn allocates memory thread block containing grid of threads to perform the large stream of calculation using parallel functions. The threads can communicate within a thread block but the blocks are distinct and CUDA function *cudaDeviceSynchronize* synchronizes thread block operations [RTO17].

5.3.2 CPU-GPU Hybrid Implementation

The developed models and algorithms are implemented on CPU and CPU-GPU hybrid computing environment. A flow chart showing the simulation process and data flow between the CPU-GPU hybrid simulation architecture is presented in Fig. 5.3. The CPU does the prepossessing and initial non-iterative steps of power flow process. That is using the available system data, Y-bus of transmission and distribution systems are formulated in CPU. The initialization of unknown vectors and initial Jacobain for TS are also evaluated in CPU. Then, the data is transferred from CPU to GPU. In the GPU, the iterative steps of power flow calculation are carried out. That is the designated functions solve for Transmission (TS) using (20), (23), and (24), and Distribution (DS) using (25) and (26). Once the TS converges, the DS sub-station voltage is updated and the DS function operates till it converges. Once, the DS function converges, the TS system load data is updated using the DS power flow and this process continues until the global integrated T&D mismatch is lower than specified tolerance and then, the final Power Flow results are transferred back to CPU from GPU for visualization.

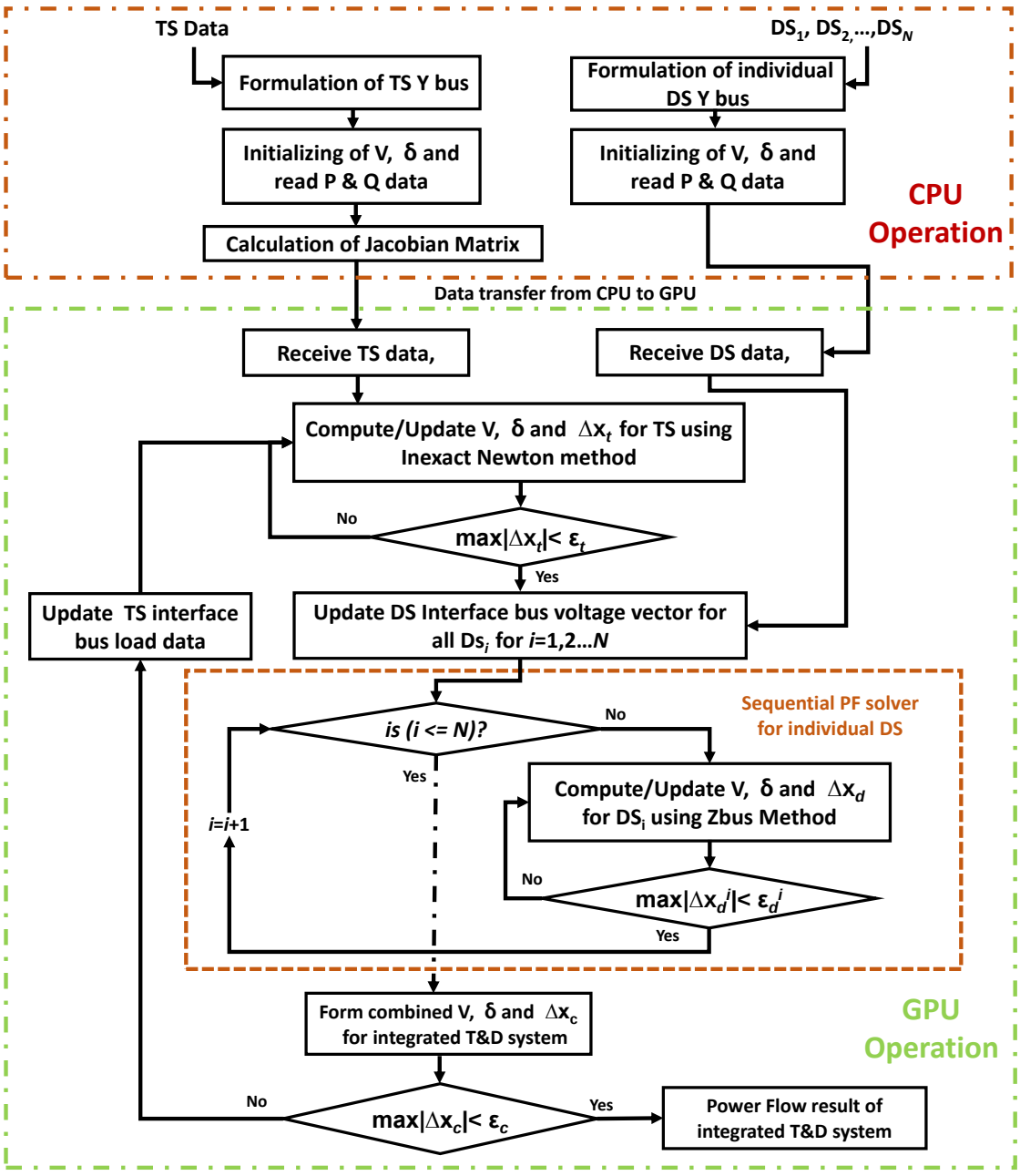

Figure 5.3: Flowchart representing CPU-GPU hybdrid simulation model of the integrated T&D system.

5.3.3 Evaluation Metrics

We adopt the following metrics to measure and evaluate the performance of the CPU and CPU-GPU based solvers.

- Solve Time (t): The elapsed time in solving the cases in CPU and CPU-GPU hybrid simulation are recording the timestamp using *cudaEventRecord()* function that returns the elapsed time between the *start* and *stop* of the kernel calls in seconds with a resolution of half a microsecond [cuC14]. The CPU runtime is recorded using CPU clock functions. The recorded timings are then compared in evaluating the performances of the solvers.

- Effective Bandwidth: The effective bandwidth is calculated using the recorded timing and accessing the details of programming data structure. For the integrated T&D system, the effective bandwidth is calculated using the formula below and is represented in units of GB/s.

$$BW_{tnd} = \frac{(I_B + O_B) \times iter}{t} \tag{5.8}$$

  where I_B and O_B are the input and output data to and from the GPU and $iter$ is the number of computational iterations.

5.4 Numerical Studies

We have tested the efficacy of the proposed architecture in three test systems ranging from small to very large scale integrated T&D systems.

5.4.1 Case 1: Small Test System

The models, solution algorithms, and hybrid CPU-GPU implementation are first tested on a small system that comprises of the IEEE 14 bus Transmission System (TS) and 123-bus Distribution System (DS) as shown in Fig. 5.4 referred as the 14-123 bus system. The IEEE 14-bus test system comprises 14 buses and 20 lines hosting 5 generators, 3 transformers, 4 capacitor banks, and 11 loads with a net

load of 260 MW (75 MVAr) which altogether is an ideal and simple approximation of the American Electric Power system. The IEEE 123-node test system operates at a nominal voltage of 4.16 kV and is characterized by three-phase overhead and underground lines, unbalanced loading with constant current, impedance, and power, four voltage regulators, shunt capacitor banks, and multiple switches with a net-connected load of 3.7 MW (1.3 MVAr). First, the transmission system and distribution system power flow convergences are independently ensured. Then, the coupled T&D model is solved using a CPU and a hybrid CPU-GPU platform using the decoupled approach. Fig. 5.5 shows the node voltage magnitudes and angles obtained from the simulation. The comparison of the same solution to its counterpart

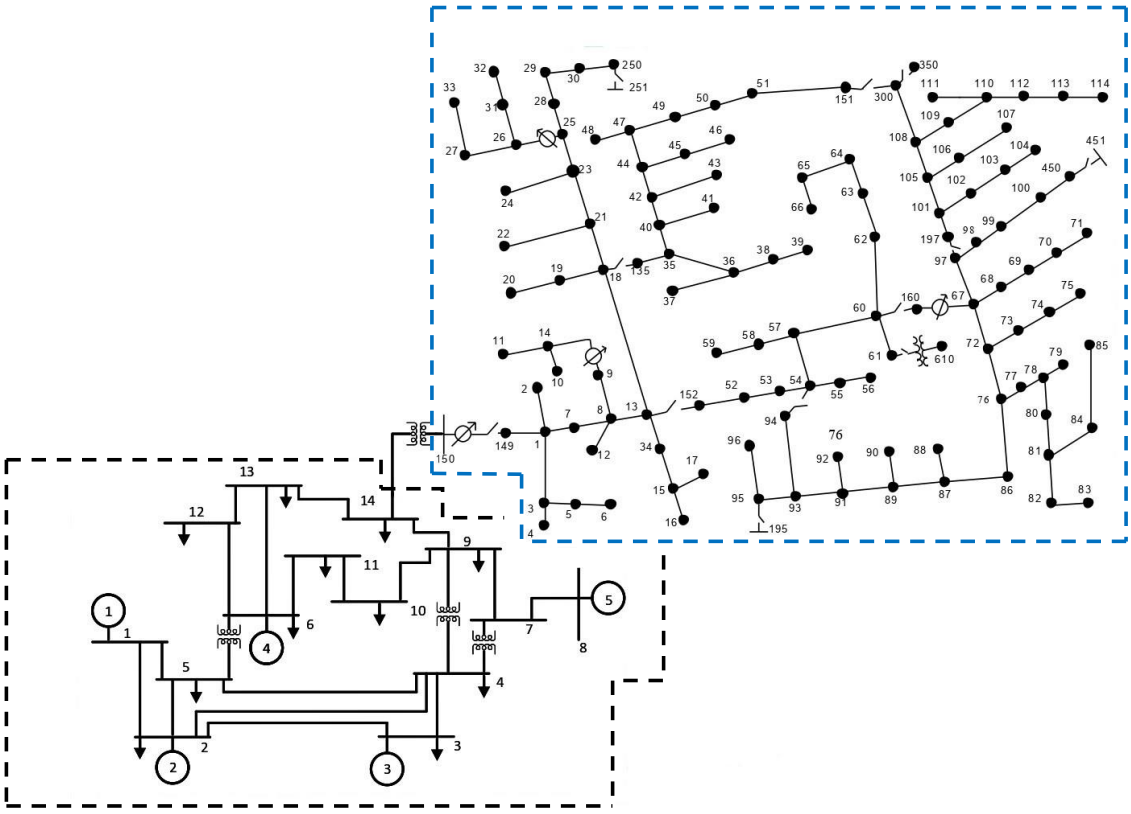

Figure 5.4: Schematic of small scale integrated T&D (14 bus transmission and 123 bus distribution system).

from CPU reveals very minimal error as seen from Fig. 5.12 and shows to outperform CPU based approach. This ensures confidence to further scale the developed approach.

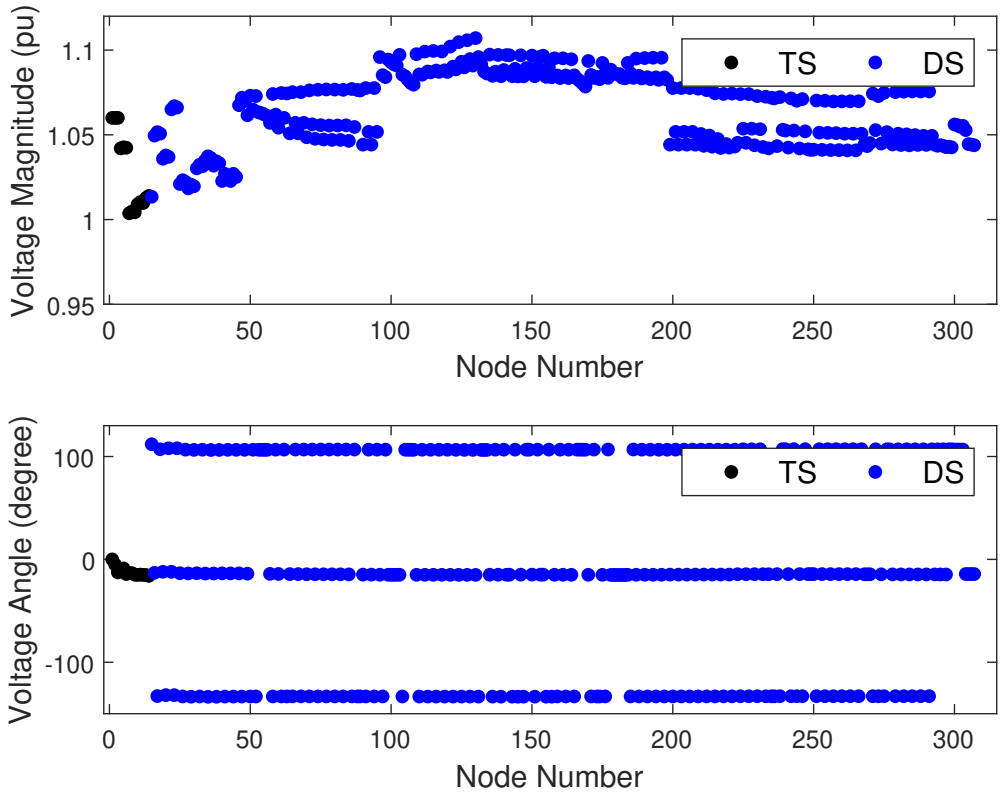

Figure 5.5: Voltage magnitude and angle of the integrated small scale T&D system (14 bus transmission and 123 bus distribution system).

5.4.2 Case 2: Large Test System

A large sized system is created by combining 2383-bus Polish transmission system (TS) and 2522 nodes distribution system (DS) that resulted in total of 6,200 nodes. The Polish network contains in total of 327 synchronous generators. The generator buses comprise 322 shunt loads and there are 1,503 active and reactive loads

measuring a net-connected load of 24,558 MW (8,144 MVAr). For the large-scale distribution case studies, a 2522-bus unbalanced distribution system is used, which is extracted from the MV-side of the IEEE 8500-node test feeder [SMP+18]. The test system has total of 3,817 single-phase nodes among which 1,413 are a load nodes. The IEEE standard load data for this feeder is modified and a load of 6.32 MW and PV of 6 MW are connected. The coupled T&D system is shown in Fig. 5.6 and is referred as 2383-2522 bus system. The resulting 6200-node system (Fig. 5.6) is then

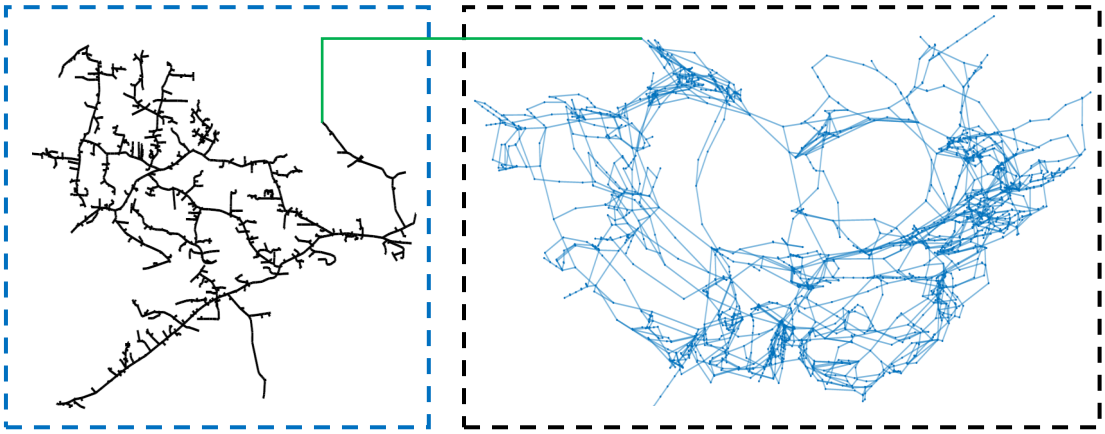

Figure 5.6: Topology of the integrated large scale T&D system (2383 bus transmission and 2522 bus distribution) .

solved in a CPU-based and CPU-GPU hybrid platform to compare the performance of voltage magnitude and angle solution on the transmission as well as distribution part of the circuit. The load flow voltage magnitude and angle obtained from the CPU-GPU hybrid platform are shown in Fig. 5.7 and Fig. 5.8, respectively.

5.4.3 Case 3: Very Large Test System

We simulated a large integrated T&D system that consists of 13,834 nodes. For this, we couple 3 instances of 2522-node unbalanced DS through 3 interface buses

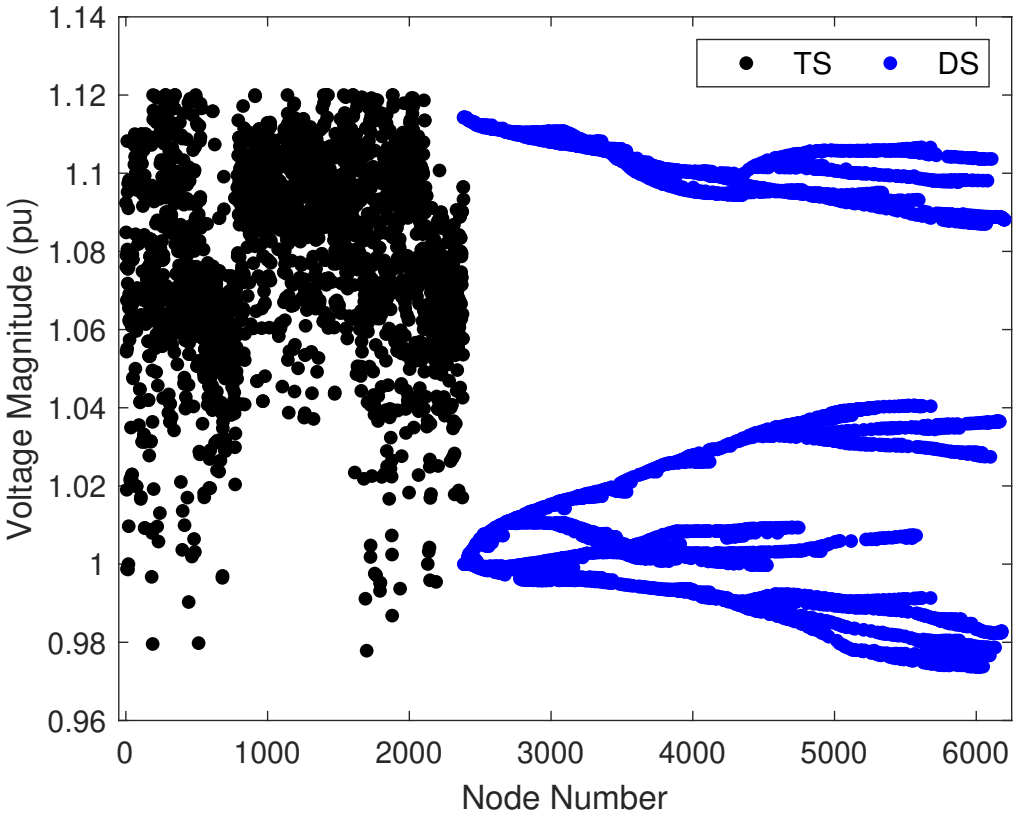

Figure 5.7: Voltage magnitude of the integrated T&D system on the large scale system with 2383 bus transmission and 2522 bus distribution.

of 2383-bus Polish TS as shown in Fig. 5.9. Fig. 5.10 and Fig. 5.11 show the nodal voltage magnitude and angle of the large scale integrated T&D system.

5.4.4 Comparative Analyses

Next, we analyze the solution accuracy, solve time, and bandwidth usage of CPU-GPU platform. Fig. 5.12 shows the error on voltage magnitude and angle (maximum of all node voltages) obtained from the CPU versus CPU-GPU architecture for the three different test feeder considered. A maximum error of 3.74×10^{-12} (p.u.) is seen on voltage magnitude on the test 13,834-node system. On the voltage angle, maximum error of $(3.30 \times 10^{-10})^{\circ}$ is observed. The errors on voltage magnitude

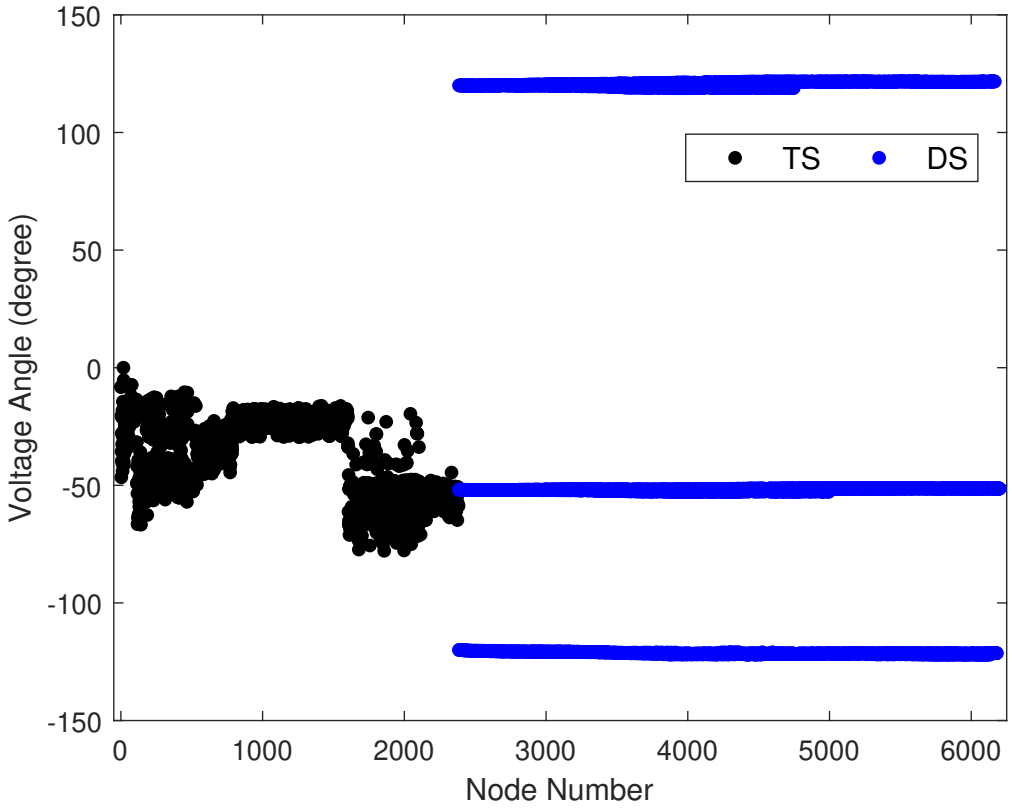

Figure 5.8: Voltage angle of the integrated T&D system on the large scale system with 2383 bus transmission and 2522 bus distribution.

as well as angle are very small and negligible. This demonstrates the accuracy of CPU-GPU based platform.

The solve time of the simulations from both CPU and CPU-GPU hybrid environment are recorded and compared in Fig. 5.13 and Table 5.1. For the small test system (i.e., the integrated system of 14-123 bus shows minimal improvement in the hybrid environment that provides only 1.15 times faster solution compared to the CPU version solve time of 3.40 s to 2.96 s by the hybrid solver as shown in the inset of Fig. 5.13. However, the computing performance of the hybrid environment are significant as the network size grows larger. For the large scale system with 6,200 nodes, the hybrid solver provides 6.67 faster solution in 114.7 s compared to 765.57 s

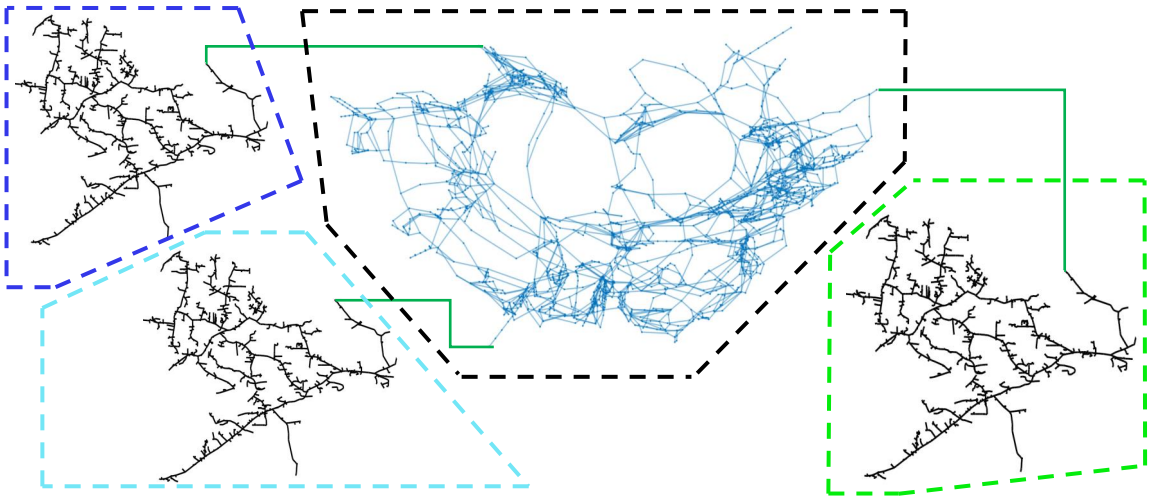

Figure 5.9: Topology of the integrated very large scale T&D system (2383 bus transmission and 3 instances of 2522 bus distribution).

by the CPU based approach. The superiority of the hybrid solver is evident from the solution of large test system with 13,000+ nodes where the hybrid platform provides a 12.05 times seed up by solving the system in 127.8 s compared to 1540.7 s by the CPU based approach.

The bandwidth for the transmission and distribution system is calculated based on (5.8). As shown in Table 5.1, the data size for a small system is 2.31 MB, and the bandwidth utilization is 0.04 GB/s. However, for the larger systems, the data size and the corresponding bandwidth improve from 1.02 GB/s, for data size 765.57 MB to 7.41 GB/s for data size 1540.70 MB, respectively. The theoretical maximum bandwidth of the utilized GPU is 112 GB/s which is much higher compared to the utilization by the 13,000+ nodes system. This result infers that the GPU system can handle even higher circuit nodes, and thus the methodology is scalable without hitting the bandwidth wall.

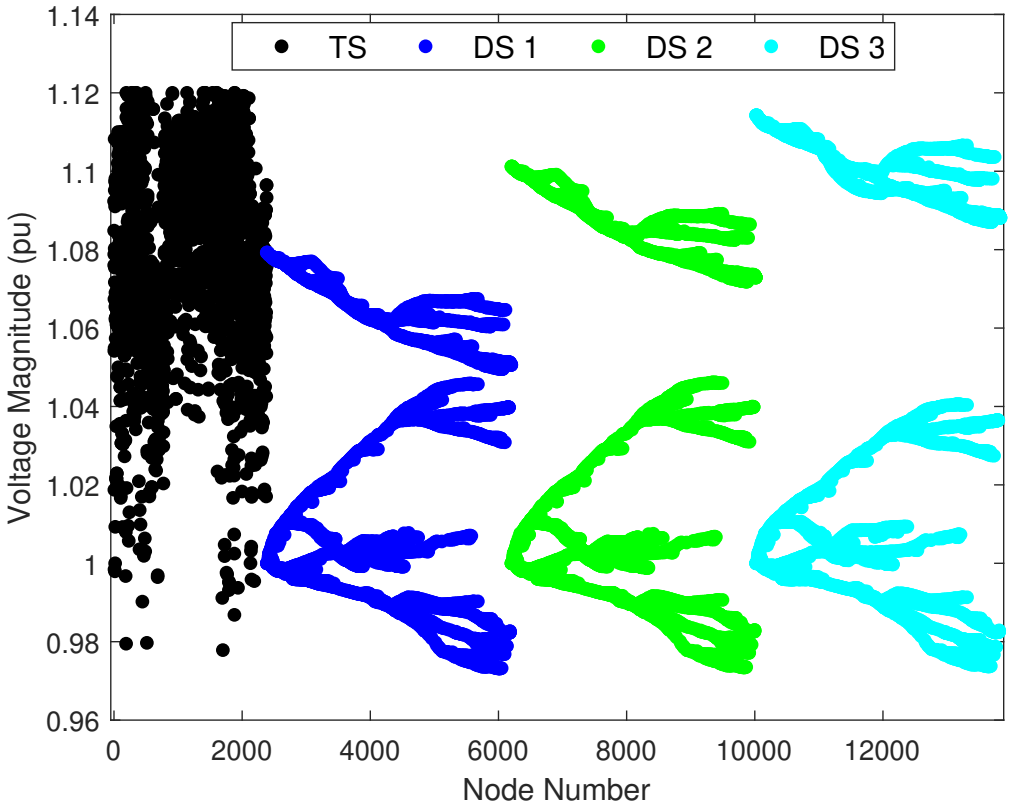

Figure 5.10: Voltage magnitude of the integrated T&D system on very large scale system (2383 bus transmission and 3 instances of 2522 bus distribution).

Table 5.1: Bandwidth and speed-up of CPU-GPU platform

	14-123	**2383-2522**	**2383-2522(3)**
Data (MB)	2.31	1,521.60	3,746.07
CPU Sim. Time (s)	3.41	765.57	1540.70
CPU-GPU Sim.Time (s)	2.96	114.70	127.84
Speed-Up	**1.15**	**6.67**	**12.05**
BW (GB/s)	**0.04**	**1.02**	**7.41**

5.5 Summary

Traditionally, the transmission systems and distribution systems are solved independently and using the off-the-shelf simulators. To the best of our knowledge, this will

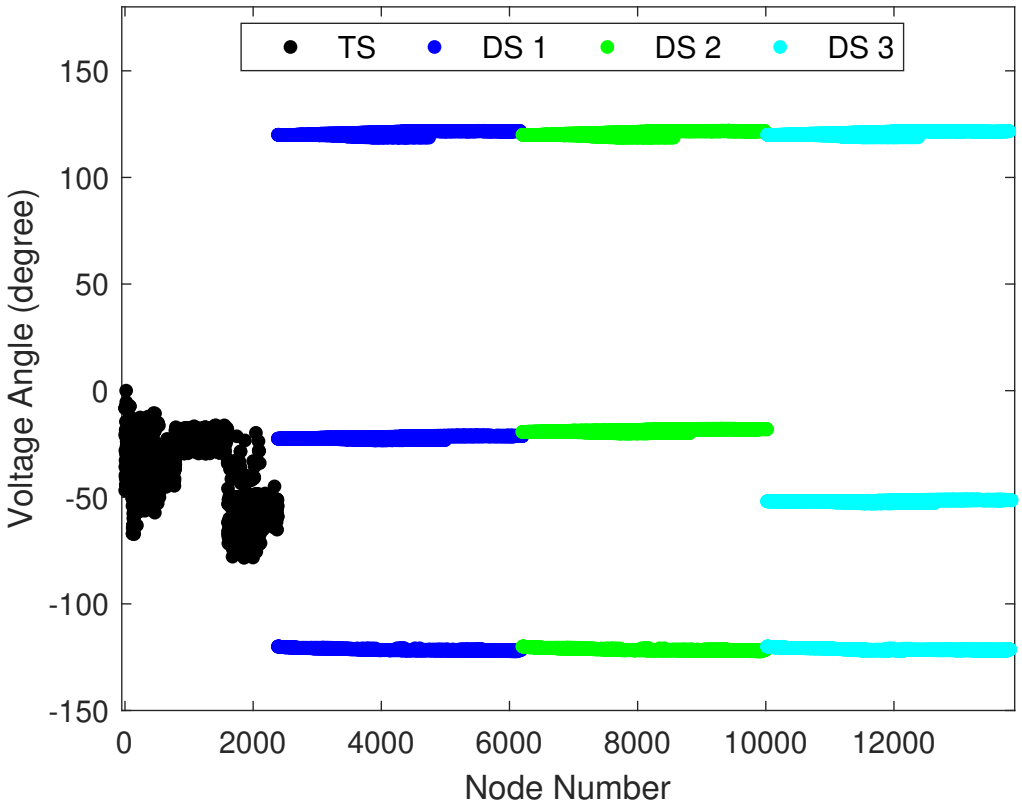

Figure 5.11: Voltage angle of the integrated T&D system (2383 bus transmission and 3 instances of 2522 bus distribution).

be the first work to implement large-scale scalable T&D simulation in GPU platform compared to the existing literature [LLY+17, HGS17, RTO17], which focused on transmission systems and [ADK12] on distribution system only, and provide a low-cost solution compared to the expensive off-the-shelf commercial tools available for integrated T&D power flow [JB18]. In this work, we formulated and tested a detailed model of transmission and distribution systems overcoming the shortcoming of existing models in the literature while showing promising outcomes in the scalability. Using the computational advantages of the inexact Newton method on the transmission side and derivative free Z-bus method on the distribution side, the developed comprehensive integrated model that is been proven to be efficient

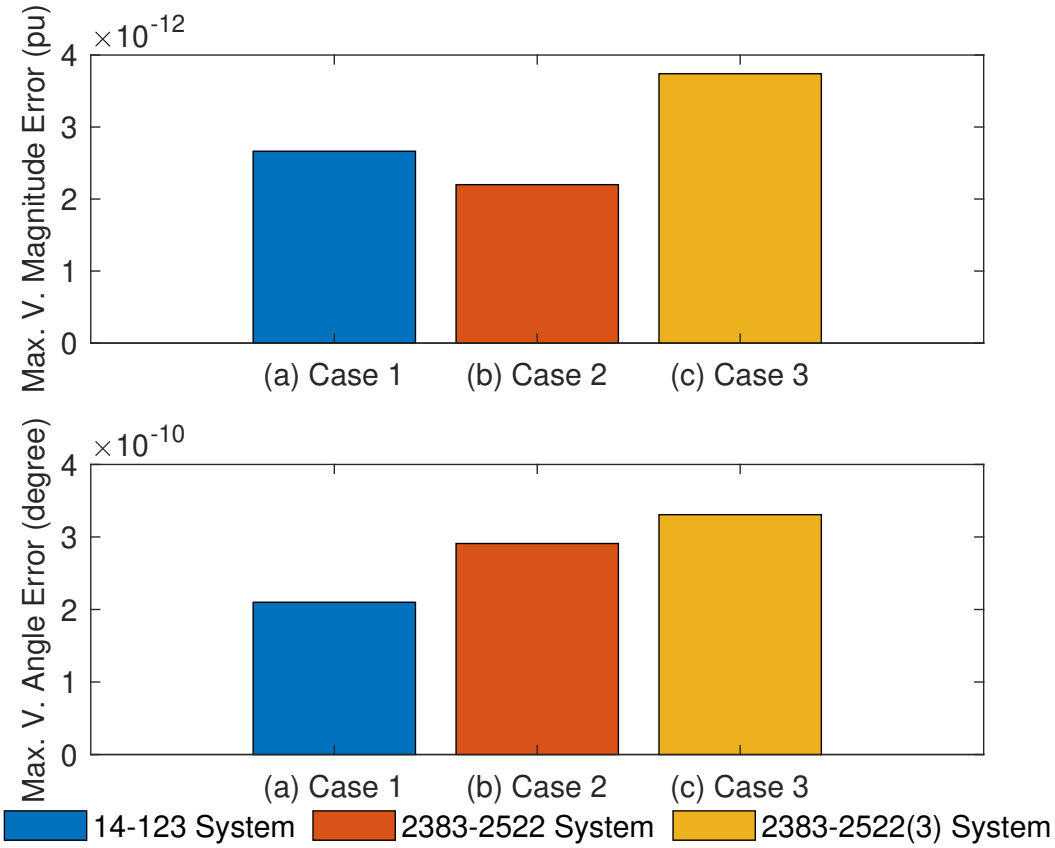

Figure 5.12: Error comparison between the CPU vs CPU-GPU platform for the integrated T&D systems.

for T&D system comprising more than 13,000 nodes. Furthermore, the model is implemented on a low-cost CPU-GPU hybrid simulation environment in achieving faster and memory efficient performance. The cost of memory transfer operation in CPU-GPU platform makes the superiority unclear in small scale system but the superiority becomes visible as the system size grows. From the simulation results and analyses, we have found that CPU-GPU based implementation outperforms CPU based solver and for the the largest integrated T&D feeder considered (2383-bus Polish transmission network and 3 instances of 2522-bus distribution network) 12 times faster performance was achieved without causing any issue in memory bandwidth. Thus, using a CPU-GPU hybrid platform , an efficient and fast PF solver is

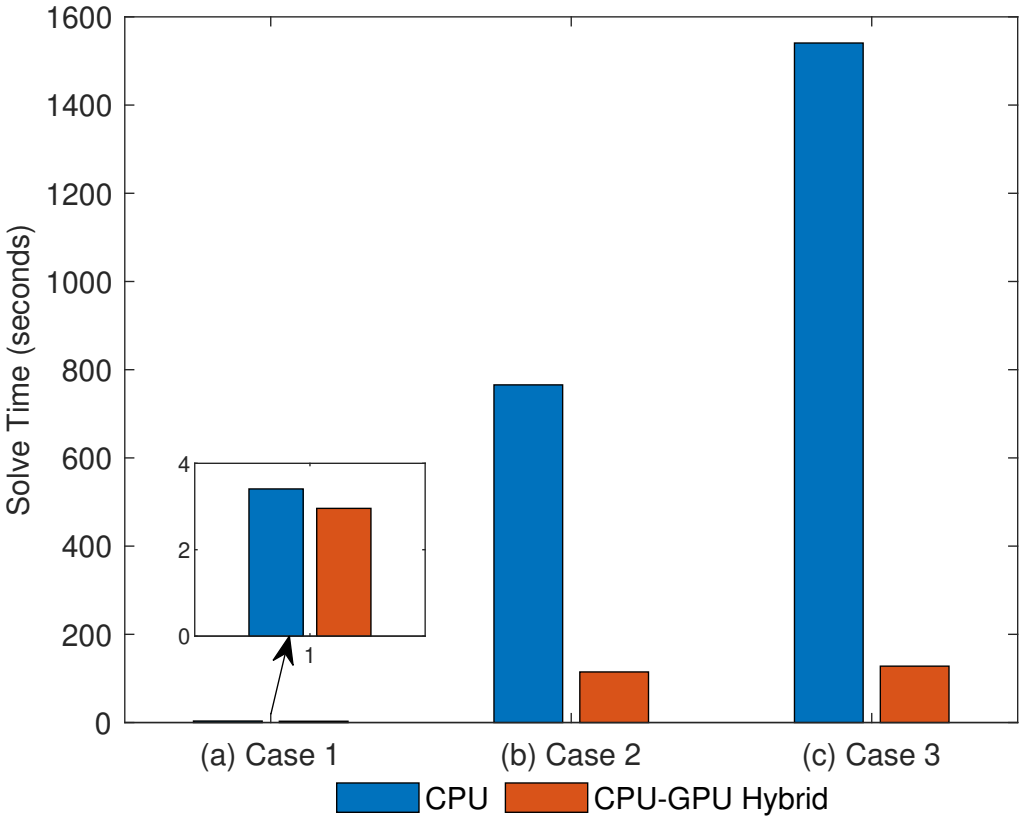

Figure 5.13: Solve time comparison between the CPU versus CPU-GPU hybrid architecture of the integrated T&D system.

developed with the intent to solve large-scale power flow model using a comprehensive mathematical model of transmission and distribution systems for steady-state analysis.

CHAPTER 6

CONCLUSION AND FUTURE WORK

This chapter provides concluding remarks and most important observations from each completed research tasks and points out the areas of future research contributions.

6.1 Network-admissible Packetized Energy Management

The work on grid-aware PEM coordinator develops a grid constricted demand dispatching scheme for efficient DER and flexible load integration to the distribution grid. Additionally, the extensive case studies provides a comprehensive performance evaluation of the developed coordination algorithm in maintaining grid states and tracking global reference set-points. The research work demonstrated the development of the smart coordinator along with the impact of packet length (in PEM), grid voltage measurement update rate, the number of voltage measurement buses, and multi-phase measurements in managing the grid voltages and in tracking the power reference signal while showing the comparison by leveraging OPF-based methods to derive time-varying nodal supply/demand capacity limits.

Based on the simulation-based analysis carried out in multiple test cases comprising of small and large scale IEEE three-phase unbalanced distribution feeders, our major observations are following:

- The grid-aware PEM coordinator performs efficiently in integrating DER and flexible load with minimal grid state violation,
- The coordinator aids in improving over-voltage conditions in the distribution grid with increased hosting.

- The tracking performance is less dependent on grid measurements and is more dependent on the packet length,
- Voltage performance depends on both grid measurements and packet length,
- Coarse packet length if complemented by fast grid measurement update rate can provide acceptable voltage performance, and
- Multi-phase measurements are essential for effective voltage control of multi-phase distribution feeders.

6.2 Integrated T&D co-simulation

With the development of coordinators in the first task to secure DER and flexible load integration, the distribution grid becomes effectively active and hence, the effect of increased penetration in the distribution grid on the transmission grid cannot be further overlooked. Therefore, we focused on the interaction of transmission and distribution grid through an integrated transmission and distribution grid simulation framework in this research task. With distribution grids becoming active systems, TS-DS in modernized power grid requires efficient models and solution methods for steady-state interactions of scalable integrated T&D systems and in this task, we handle that requirement through comprehensive mathematical model (including three-phase circuit components of distribution feeders) to study T&D interactions in detail.

Based on the simulation-based analysis carried out through multiple test cases of variable scale comprising of small scale IEEE transmission and distribution test feeders, our major contributions and observations are following:

- In the development of integrated T&D simulation framework, at first, we have developed a decoupled approach for solving T&D co-simulation for benchmarking purpose with a collaborator-developed unified approach.
- Since in the literature a phasor-based benchmark to validate decoupled approach was lacking, we present the initial results obtained towards building a benchmark with corresponding unified T&D model.
- The accuracy of a decoupled approach is compared to the unified solution and for the initially developed small-scale systems present very similar results and hence, provides the confidence for scalability.

6.3 GPU based large-scale Integrated T&D co-simulation

In the third and final work, building upon the developed decoupled T&D co-simulation framework in the previous task, we formulated and tested a detailed model of large-scale transmission and distribution systems overcoming the shortcoming of existing models in the literature while showing promising outcomes in the scalability on a CPU-GPU hybrid framework for efficient and fast PF solver.

- Using the computationally advantageous mathematical methods to build TS & DS network, the developed comprehensive integrated model is been proven to be efficient and provides accurate results for large-scale T&D system.
- Furthermore, the model is implemented on a low-cost CPU-GPU hybrid simulation environment in achieving faster and memory efficient performance.
- The CPU-GPU platform showcases superior performance in simulation runtime and memory usage in solving large-scale integrated systems.

6.4 Future work

Now, with the completed research tasks, we have efficiently developed a grid-aware demand dispatch scheme; capable of actively monitoring and controlling grid states on the distribution side and in the other block; a simulation platform to effectively monitor and simulate the interactions between transmission and distribution grid collectively to study this increased interaction.

- In the development of network-admissible PEM based network coordinator, at finest we have used a 2-second measurement update rate. However, in real-world implementations the effects of latency and refresh rate in higher layers of the communication network could effectively take longer than 2 seconds and hence, a closer look on the effect of communication delay on such measurement update rate is of importance and this could be an important contribution in this project for more efficient DER coordination.
- In the integrated T&D co-simulation, further research could be performed on the unified simulation of T&D grids using a common simulation method that is capable of all types of system buses.
- In the GPU based large-scale integrated T&D co-simulation, further research is required to engage the full computational capabilities of the GPU in building a working PF solver based solely on GPU.

At the present status of the work, the working blocks are working perfectly on their own and in the future work, we would effectively integrate the blocks of distribution side grid-aware PEM scheme in the integrated T&D grid framework to study the impact of such coordination in real-time.

BIBLIOGRAPHY

[ADK12] D. Ablakovic, I. Dzafic, and S. Kecici. Parallelization of radial three-phase distribution power flow using GPU. In *Proc. 3rd IEEE PES Innovative Smart Grid Technologies Europe (ISGT Europe)*, pages 1–7, Oct 2012.

[AEHH+18] Mads Almassalkhi, Luis Duffaut Espinosa, Paul D. H. Hines, Jeff Frolik, Sumit Paudyal, and Mahraz Amini. *Asynchronous Coordination of Distributed Energy Resources with Packetized Energy Management*, pages 333–361. Springer New York, New York, NY, 2018.

[AFH17] M. Almassalkhi, J. Frolik, and P. Hines. Packetized energy management: Asynchronous and anonymous coordination of thermostatically controlled loads. In *2017 American Control Conference (ACC)*, pages 1431–1437, May 2017.

[AVC15] Petros Aristidou and Thierry Van Cutsem. A parallel processing approach to dynamic simulations of combined transmission and distribution systems. *International Journal of Electrical Power Energy Systems*, 72, 11 2015.

[BA17] K. Balasubramaniam and S. Abhyankar. A combined transmission and distribution system co-simulation framework for assessing the impact of volt/var control on transmission system. In *Proc. IEEE Power Energy Society General Meeting*, pages 1–5, July 2017.

[BBDZ18] Kyri Baker, Andrey Bernstein, Emiliano Dall'Anese, and Changhong Zhao. Network-cognizant voltage droop control for distribution grids. *IEEE Transactions on Power Systems*, 33(2):2098–2108, 2018.

[BCCN00] E. Bompard, E. Carpaneto, G. Chicco, and R. Napoli. Convergence of the backward/forward sweep method for the load-flow analysis of radial distribution systems. *International Journal of Electrical Power Energy Systems*, 22(7):521 – 530, 2000.

[BG18a] M. Bazrafshan and N. Gatsis. Comprehensive modeling of three-phase distribution systems via the bus admittance matrix. *IEEE Transactions on Power Systems*, 33(2):2015–2029, March 2018.

[BG18b] M. Bazrafshan and N. Gatsis. Convergence of the Z-Bus Method for Three-Phase Distribution Load-Flow with ZIP Load. *IEEE Transactions on Power Systems*, 33(1):153–165, Jan 2018.

[BGMEA76] K.A. Birt, J.J. Graffy, J.D. McDonald, and A.H. El-Abiad. Three phase load flow program. *IEEE Transactions on Power Apparatus and Systems*, 95(1):59–65, 1976.

[BKOA21] Sarnaduti Brahma, Adil Khurram, Hamid Ossareh, and Mads Almassalkhi. Optimal frequency regulation using packetized energy management, 2021. Under review at: https://arxiv.org/abs/2107.12939.

[CCH+91] T. Chen, M Chen, K Hwang, P. Kotas, and E. A. Chebli. Distribution system power flow analysis-a rigid approach. *IEEE Transactions on Power Delivery*, 6(3):1146–1152, July 1991.

[CCW07] G. W. Chang, S. Y. Chu, and H. L. Wang. An improved backward/forward sweep load flow algorithm for radial distribution systems. *IEEE Transactions on Power Systems*, 22(2):882–884, May 2007.

[CDZL20] X. Chen, E. Dall'Anese, C. Zhao, and N. Li. Aggregate power flexibility in unbalanced distribution systems. *IEEE Transactions on Smart Grid*, 11(1):258–269, 2020.

[CFO03] R.M. Ciric, A.P. Feltrin, and L.F. Ochoa. Power flow in four-wire distribution networks-general approach. *IEEE Transactions on Power Systems*, 18(4):1283–1290, 2003.

[CH10] Duncan S Callaway and Ian A Hiskens. Achieving controllability of electric loads. *Proceedings of the IEEE*, 99(1):184–199, 2010.

[CH11] D. S. Callaway and I. A. Hiskens. Achieving controllability of electric loads. *Proceedings of the IEEE*, 99(1):184–199, Jan 2011.

[CS95] C. S. Cheng and D. Shirmohammadi. A three-phase power flow method for real-time distribution system analysis. *IEEE Transactions on Power Systems*, 10(2):671–679, May 1995.

[cuC14] *Professional CUDA C Programming*. Wrox Press Ltd., GBR, 1st edition, 2014.

[CZDK14] H. Chiang, T. Zhao, J. Deng, and K. Koyanagi. Convergence/divergence analysis of implicit Z-bus power flow for general distribution networks. In *2014 IEEE International Symposium on Circuits and Systems (ISCAS)*, pages 1808–1811, June 2014.

[DA20] L. A. Duffaut Espinosa and M. Almassalkhi. A packetized energy management macromodel with quality of service guarantees for demand-side resources. *IEEE Transactions on Power Systems*, 35(5):3660–3670, 2020.

[DMJK08] Min Dai, Mohammad Nanda Marwali, Jin-Woo Jung, and Ali Keyhani. Power flow control of a single distributed generation unit. *IEEE Transactions on Power Electronics*, 23(1):343–352, 2008.

[dMP99] V. M. da Costa, N. Martins, and J. L. R. Pereira. Developments in the newton raphson power flow formulation based on current injections. *IEEE Transactions on Power Systems*, 14(4):1320–1326, Nov 1999.

[EPR] EPRI. Simulation Tool–OpenDSS. http://smartgrid.epri.com/SimulationTool.aspx.

[FL13] M. Farivar and S.H. Low. Branch flow model: Relaxations and convexification -Part I. *IEEE Transactions on Power Systems*, 28(3):2554–2564, Aug. 2013.

[FVS11] Jianbin Fang, Ana Lucia Varbanescu, and Henk Sips. A comprehensive performance comparison of CUDA and OpenCL. In *Proc. International Conference on Parallel Processing*, pages 216–225, 2011.

[Gar10] N. Garcia. Parallel power flow solutions using a biconjugate gradient algorithm and a newton method: A GPU-based approach. In *Proc. IEEE PES General Meeting*, pages 1–4, July 2010.

[GD99] S. Ghosh and D. Das. Method for load-flow solution of radial distribution networks. *IEE Proceedings - Generation, Transmission and Distribution*, 146(6):641–648, Nov 1999.

[GJY+12] C. Guo, B. Jiang, H. Yuan, Z. Yang, L. Wang, and S. Ren. Performance comparisons of parallel power flow solvers on GPU system. In *Proc. IEEE International Conference on Embedded and Real-Time Computing Systems and Applications*, pages 232–239, Aug 2012.

[GPC+00] P. A. N. Garcia, J. L. R. Pereira, S. Carneiro, V. M. da Costa, and N. Martins. Three-phase power flow calculations using the current injection method. *IEEE Transactions on Power Systems*, 15(2):508–514, May 2000.

[GZZ+20] Yi Guo, Xinyang Zhou, Changhong Zhao, Yue Chen, Tyler Summers, and Lijun Chen. Solving optimal power flow for distribution networks with state estimation feedback. In *Proc. American Control Conference*, pages 3148–3155, 2020.

[HFD+17] R. Huang, R. Fan, J. Daily, A. Fisher, and J. Fuller. Open-source framework for power system transmission and distribution dynamics co-simulation. *IET Generation, Transmission Distribution*, 11(12):3152–3162, 2017.

[HGS17] T. Huang, Q. Guo, and H. Sun. A distributed computing platform supporting power system security knowledge discovery based on online simulation. *IEEE Transactions on Smart Grid*, 8(3):1513–1524, May 2017.

[HV17] Q. Huang and V. Vittal. Integrated transmission and distribution system power flow and dynamic simulation using mixed three-sequence/three-phase modeling. *IEEE Transactions on Power Systems*, 32(5):3704–3714, Sep. 2017.

[ISPK21] Adedoyin Inaolaji, Alper Savasci, Sumit Paudyal, and Sukumar Kamalasadan. Accuracy of phase-decoupled and phase-coupled distribution grid power flow models. In *Proc. IEEE Power Energy Society Innovative Smart Grid Technologies Conference (ISGT)*, pages 1–5, 2021.

[JB18] V. Jalili-Marandi and J. Bélanger. Real-time transient stability simulation of confederated transmission-distribution power grids with more than 100,000 nodes. In *Proc. IEEE Power Energy Society General Meeting*, pages 1–5, Aug 2018.

[JDS+09] V. Jalili-Marandi, V. Dinavahi, K. Strunz, J. A. Martinez, and A. Ramirez. Interfacing techniques for transient stability and electromagnetic transient programs IEEE task force on interfacing techniques for simulation tools. *IEEE Transactions on Power Delivery*, 24(4):2385–2395, Oct 2009.

[JMW16] N. Jayasekara, M. A. S. Masoum, and P. J. Wolfs. Optimal operation of distributed energy storage systems to improve distribution network load and generation hosting capability. *IEEE Transactions on Sustainable Energy*, 7(1):250–261, 2016.

[JPB+16] H. Jain, A. Parchure, R. P. Broadwater, M. Dilek, and J. Woyak. Three-phase dynamic simulation of power systems using combined transmission and distribution system models. *IEEE Transactions on Power Systems*, 31(6):4517–4524, Nov 2016.

[JWZS14] Y. Ju, W. Wu, B. Zhang, and H. Sun. An extension of FBS three-phase power flow for handling pv nodes in active distribution networks. *IEEE Transactions on Smart Grid*, 5(4):1547–1555, July 2014.

[Ker84] W. H. Kersting. A method to teach the design and operation of a distribution system. *IEEE Transactions on Power Apparatus and Systems*, PAS-103(7):1945–1952, July 1984.

[KH10] David B. Kirk and Wen-mei W. Hwu. *Programming Massively Parallel Processors: A Hands-on Approach*. Applications of GPU Computing Series. Morgan Kaufmann Publishers, Burlington, MA, 2010.

[KM76] WH Kersting and DL Mendive. An application of ladder theory to the solution of three-phase radial load-flow problem. *IEEE Transactions on Power Apparatus and Systems*, 98(7):1060–1067, 1976.

[KPAew] Mohammad Asif Iqbal Khan, Sumit Paudyal, and Mads Almassalkh. Network-admissible demand dispatch with packetized energy management. *IEEE Transactions on Smart Grid*, 2021 [Under Review].

[KSPK19] Mohammad Asif Iqbal Khan, Arun Suresh, Sumit Paudyal, and Sukumar Kamalasadan. Decoupled and unified approaches for solving transmission and distribution co-simulations. In *Proc. North American Power Symposium (NAPS)*, pages 1–6, 2019.

[KSS08] Dina Khaniya, Anurag K. Srivastava, and Noel N. Schulz. Distribution power flow for multiphase meshed or radial systems. In *2008 40th North American Power Symposium*, pages 1–5, 2008.

[KZGB16] V. Kekatos, L. Zhang, G. B. Giannakis, and R. Baldick. Voltage regulation algorithms for multiphase power distribution grids. *IEEE Transactions on Power Systems*, 31(5):3913–3923, 2016.

[LBT+19] C. Le Floch, S. Bansal, C. J. Tomlin, S. J. Moura, and M. N. Zeilinger. Plug-and-play model predictive control for load shaping and voltage control in smart grids. *IEEE Transactions on Smart Grid*, 10(3):2334–2344, 2019.

[LL15] X. Li and F. Li. Gpu-based two-step preconditioning for conjugate gradient method in power flow. In *Proc. IEEE Power Energy Society General Meeting*, pages 1–5, July 2015.

[LLY+17] X. Li, F. Li, H. Yuan, H. Cui, and Q. Hu. GPU-based fast decoupled power flow with preconditioned iterative solver and inexact newton method. *IEEE Transactions on Power Systems*, 32(4):2695–2703, July 2017.

[LM19] H. Liao and J. V. Milanovic. Flexibility exchange strategy to facilitate congestion and voltage profile management in power networks. *IEEE Transactions on Smart Grid*, 10(5):4786–4794, Sep. 2019.

[LN97] H. Le Nguyen. Newton-raphson method in complex form [power system load flow analysis]. *IEEE Transactions on Power Systems*, 12(3):1355–1359, 1997.

[LSCT99] Whei-Min Lin, Yuh-Sheng Su, Hong-Chan Chin, and Jen-Hao Teng. Three-phase unbalanced distribution power flow solutions with minimum data preparation. *IEEE Transactions on Power Systems*, 14(3):1178–1183, 1999.

[LWSG15] Z. Li, J. Wang, H. Sun, and Q. Guo. Transmission contingency analysis based on integrated transmission and distribution power flow in smart grid. *IEEE Transactions on Power Systems*, 30(6):3356–3367, Nov 2015.

[LWT13] X. Liu, H. Wang, and S. X. . Tan. Parallel power grid analysis using preconditioned gmres solver on CPU-GPU platforms. In *Proc. IEEE/ACM International Conference on Computer-Aided Design (ICCAD)*, pages 561–568, Nov 2013.

[MGP16] B. Muruganantham, R. Gnanadass, and N. P. Padhy. Performance analysis and comparison of load flow methods in a practical distribution system. In *2016 National Power Systems Conference (NPSC)*, pages 1–6, Dec 2016.

[Mil10] Federico Milano. *Power Flow Analysis*, pages 61–101. Springer Berlin Heidelberg, Berlin, Heidelberg, 2010.

[MKG+07] G. Mueller, P. Komarnicki, I. Golub, Z. Styczynski, C. Dzienis, and J. Blumschein. Pmu placement method based on decoupled newton power flow and sensitivity analysis. In *2007 9th International Conference on Electrical Power Quality and Utilisation*, pages 1–5, 2007.

[MR19] Daniel Molzahn and Line A Roald. Grid-aware versus grid-agnostic distribution system control: A method for certifying engineering constraint satisfaction. In *Proceedings of the 52nd Hawaii International Conference on System Sciences*, 2019.

[MT09] J. M. Marinho and G. Taranto. A hybrid three-phase single-phase power flow formulation. In *Proc. IEEE Power Energy Society General Meeting*, pages 1–1, July 2009.

[NA19a] N. Nazir and M. Almassalkhi. Convex inner approximation of the feeder hosting capacity limits on dispatchable demand. In *2019 IEEE 58th Conference on Decision and Control (CDC)*, pages 4858–4864, 2019.

[NA19b] Nawaf Nazir and Mads Almassalkhi. Grid-aware aggregation and real-time disaggregation of distributed energy resources in radial networks. *arXiv preprint arXiv:1907.06709*, 2019.

[NVI10] NVIDIA Corporation. NVIDIA CUDA C programming guide, 2010. Version 3.2.

[PAGV14] F. J. Plumier, P. Aristidou, C. Geuzaine, and T. Van Cutsem. A relaxation scheme to combine phasor-mode and electromagnetic transients simulations. In *Proc. Power Systems Computation Conference*, pages 1–7, Aug 2014.

[PAP+04] D.R.R. Penido, L.R. Araujo, J.L.R. Pereira, P.A.N. Garcia, and S. Carneiro. Four wire newton-raphson power flow based on the current injection method. In *IEEE PES Power Systems Conference and Exposition, 2004.*, pages 239–242 vol.1, 2004.

[PBD20] Miguel Picallo, Saverio Bolognani, and Florian Dörfler. Closing the loop: Dynamic state estimation and feedback optimization of power grids. *Electric Power Systems Research*, 189:106753, 2020.

[Rah08] S. Rahman. Framework for a resilient and environment-friendly microgrid with demand-side participation. In *2008 IEEE Power and Energy Society General Meeting - Conversion and Delivery of Electrical Energy in the 21st Century*, pages 1–1, July 2008.

[RAW21] Yuri R. Rodrigues, Morad Mohamed Abdelmageed Abdelaziz, and Liwei Wang. D-PMU based distributed voltage and frequency control for DERs in islanded microgrids. *IEEE Transactions on Sustainable Energy*, 12(1):451–468, 2021.

[RB88] D. Rajicic and A. Bose. A modification to the fast decoupled power flow for networks with high R/X ratios. *IEEE Transactions on Power Systems*, 3(2):743–746, May 1988.

[RDM17] Matthew J. Reno, Jeremiah Deboever, and Barry Mather. Motivation and requirements for quasi-static time series (QSTS) for distribution system analysis. In *Proc. IEEE Power Energy Society General Meeting*, pages 1–5, 2017.

[RTO17] V. Roberge, M. Tarbouchi, and F. Okou. Parallel power flow on graphics processing units for concurrent evaluation of many networks. *IEEE Transactions on Smart Grid*, 8(4):1639–1648, July 2017.

[SA74] B. Stott and O. Alsac. Fast decoupled load flow. *IEEE Transactions on Power Apparatus and Systems*, PAS-93(3):859–869, May 1974.

[SAM19] C. Spanias, P. Aristidou, and M. Michaelides. Demand-side volt/var/watt regulation for effective voltage control in distribution grids. In *2019 IEEE PES Innovative Smart Grid Technologies Europe (ISGT-Europe)*, pages 1–5, 2019.

[SCL+12] Ching-Lung Su, Po-Yu Chen, Chun-Chieh Lan, Long-Sheng Huang, and Kuo-Hsuan Wu. Overview and comparison of OpenCL and CUDA technology for GPGPU. In *Proc. IEEE Asia Pacific Conference on Circuits and Systems*, pages 448–451, 2012.

[SGZ+15] H. Sun, Q. Guo, B. Zhang, Y. Guo, Z. Li, and J. Wang. Master–slave-splitting based distributed global power flow method for integrated transmission and distribution analysis. *IEEE Transactions on Smart Grid*, 6(3):1484–1492, May 2015.

[SKD20] Rabayet Sadnan, Gayathri Krishnamoorthy, and Anamika Dubey. Transmission and distribution (T&D) quasi-static co-simulation: Analysis and comparison of T&D coupling strength. *IEEE Access*, 8:124007–124019, 2020.

[SMP+18] K. P. Schneider, B. A. Mather, B. C. Pal, C.-W. Ten, G. J. Shirek, H. Zhu, J. C. Fuller, J. L. R. Pereira, L. F. Ochoa, L. R. de Araujo, R. C. Dugan, S. Matthias, S. Paudyal, T. E. McDermott, and W. Kersting. Analytic considerations and design basis for the ieee distribution test feeders. *IEEE Transactions on Power Systems*, 33(3):3181–3188, 2018.

[TC02] Jen-Hao Teng and Chuo-Yean Chang. A novel and fast three-phase load flow for unbalanced radial distribution systems. *IEEE Transactions on Power Systems*, 17(4):1238–1244, 2002.

[Ten03] Jen-Hao Teng. A direct approach for distribution system load flow solutions. *IEEE Transactions on power delivery*, 18(3):882–887, 2003.

[TGK19] A. Thakallapelli, S. Ghosh, and S. Kamalasadan. Development and applicability of online passivity enforced wide-band multi-port equivalents for hybrid transient simulation. *IEEE Transactions on Power Systems*, 34(3):2302–2311, May 2019.

[TH67] W. F. Tinney and C. E. Hart. Power flow solution by newton's method. *IEEE Transactions on Power Apparatus and Systems*, PAS-86(11):1449–1460, Nov 1967.

[U.] U. S. Department of Energy at PNNL. GridLAB-D, Power Distribution Simulation Software. [Online]. Available: http://www.gridlabd.org/.

[VKA18] Ramakrishnan Venkatraman, Siddhartha Kumar Khaitan, and Venkataramana Ajjarapu. Dynamic co-simulation methods for combined transmission-distribution system and integration time step impact on convergence. *CoRR*, abs/1801.01185, 2018.

[WBP+19] J. Wang, G. R. Bharati, S. Paudyal, O. Ceylan, B. P. Bhattarai, and K. S. Myers. Coordinated electric vehicle charging with reactive power support to distribution grids. *IEEE Transactions on Industrial Informatics*, 15(1):54–63, 2019.

[WCGW16] S. Wang, S. Chen, L. Ge, and L. Wu. Distributed generation hosting capacity evaluation for distribution systems considering the robust optimal operation of oltc and svc. *IEEE Transactions on Sustainable Energy*, 7(3):1111–1123, 2016.

[WCK+19] Z. Wang, A. Chakrabortty, C. T. Kelley, X. Feng, and P. Franzon. Improved numerical methodologies on power system dynamic simulation using gpu implementation. In *Proc. IEEE Power Energy Society Innovative Smart Grid Technologies Conference (ISGT)*, pages 1–5, Feb 2019.

[XFC13] Xue Li, Fangxing Li, and J. M. Clark. Exploration of multifrontal method with gpu in power flow computation. In *Proc. IEEE Power Energy Society General Meeting*, pages 1–5, July 2013.

[ZBC+17] G. Zhou, R. Bo, L. Chien, X. Zhang, F. Shi, C. Xu, and Y. Feng. Gpu-based batch lu-factorization solver for concurrent analysis of massive power flows. *IEEE Transactions on Power Systems*, 32(6):4975–4977, Nov 2017.

[ZBC+18] G. Zhou, R. Bo, L. Chien, X. Zhang, S. Yang, and D. Su. GPU-accelerated algorithm for on-line probabilistic power flow. In *Proc. IEEE Power Energy Society General Meeting (PESGM)*, pages 1–1, Aug 2018.

[ZC95] Ray D Zimmerman and Hsiao-Dong Chiang. Fast decoupled power flow for unbalanced radial distribution systems. *IEEE Transactions on Power Systems*, 10(4):2045–2052, 1995.

[ZC97] Fan Zhang and Carol S Cheng. A modified newton method for radial distribution system power flow analysis. *IEEE Transactions on Power Systems*, 12(1):389–397, 1997.

[ZFB+17] G. Zhou, Y. Feng, R. Bo, L. Chien, X. Zhang, Y. Lang, Y. Jia, and Z. Chen. Gpu-accelerated batch-acpf solution for n-1 static security analysis. *IEEE Transactions on Smart Grid*, 8(3):1406–1416, May 2017.

[ZGW+13] Y. Zhang, A. M. Gole, W. Wu, B. Zhang, and H. Sun. Development and analysis of applicability of a hybrid transient simulation platform combining TSA and EMT elements. *IEEE Transactions on Power Systems*, 28(1):357–366, Feb 2013.

[Zha96] Xiao-Ping Zhang. Fast three phase load flow methods. *IEEE Transactions on Power Systems*, 11(3):1547–1554, 1996.

[ZT02] Y Zhu and Kevin Tomsovic. Adaptive power flow method for distribution systems with dispersed generation. *IEEE Transactions on Power Delivery*, 17(3):822–827, 2002.

VITA

MOHAMMAD ASIF IQBAL KHAN

December 1, 1989	Born, Dhaka, Bangladesh
2011	B.S., Electrical and Electronic Engineering American International University-Bangladesh Dhaka, Bangladesh
2014	M.S., Computer Science Electrical Power Engineering Aachen, Germany

PUBLICATIONS AND PRESENTATIONS

Mohammad Asif Iqbal Khan; Sumit Paudyal; Mads R. Almassalkhi, *Network-Admissible Demand Dispatch with Packetized Energy Management (Submitted)*, IEEE Transactions on Power Systems

Mohammad Asif Iqbal Khan; Sumit Paudyal; Mads R. Almassalkhi, *Performance Evaluation of Network-Admissible Demand Dispatch in Multi-Phase Distribution Grids (Accepted)*, 2022 IREP Bulk Power System Dynamics and Control Symposium

Mohammad Asif Iqbal Khan; Sumit Paudyal; Sukumar Kamalasadan, *Efficient Large-Scale Simulation of Integrated Transmission and Distribution Systems (Accepted)*, IEEE Kansas Power and Energy Conference, 2022

Mohammad Asif Iqbal Khan; Sumit Paudyal; Sukumar Kamalasadan, Abhi D. *GPU-based Efficient Real-Time Large-Scale Unified Transmission and Distribution Grid Simulation (Submitted)*, IEEE Transactions on Smart Grids

Mohammad Asif Iqbal Khan; Arun Suresh; Sumit Paudyal; Sukumar Kamalasadan; *Decoupled and Unified Approaches for Solving Transmission and Distribution Co-Simulations*, 2019 North American Power Symposium (NAPS),13-15 Oct. 2019.

Jingyuan Wang; Emin Y. Ucer; Sumit Paudyal; Mithat C. Kisacikoglu; Mohammad A. I. Khan**,** *Distribution Grid Voltage Support with Four Quadrant Control of Electric Vehicle Chargers*, 2019 IEEE Power Energy Society General Meeting (PESGM), 4-8 Aug. 2019.

Fetnando B. dos Reis; Kapil Duwadi; Robert Foutney; Reinaldo Tonkoski; Timothy M. Hansen; Mohammad Asif Iqbal Khan; Sumit Paudyal; *Impact of Residential*

Load Models for Overvoltage Prevention Studies in PV-Rich LV Grids, 2019 IEEE Milan PowerTech, 23-27 June 2019.

Hemanth Kumar Vemprala; Mohammad Asif Iqbal Khan; Sumit Paudyal; *Open-source Poly-phase Distribution System Power Flow Analysis Tool (DxFlow)*, 2019 IEEE International Conference on Electro Information Technology (EIT), 20-22 May 2019.